Revue des Composites et des Matériaux Avancés-Journal of Composite and Advanced Materials
Vol. 36, No. 4, August, 2026, pp. 905-928
Journal homepage: http://iieta.org/journals/rcma

Optimizing Waste Glass Powder Content for Chloride-Exposed Reinforced Concrete: Mechanical Performance, Microstructural Characterization, and Corrosion Assessment

Aula Jamal Hasan Alansare[1*], Agusril Syamsir[2,3], Nor Hazwani Nor Khalid[2]

[1] College of Graduate Studies, Universiti Tenaga Nasional, Kajang 43000, Malaysia
[2] Civil Engineering Department, Institute of Energy Infrastructure (IEI), Universiti Tenaga National, Kajang 43000, Malaysia
[3] Faculty of Engineering, Universitas Putra Indonesia YPTK, Padang 25145, Indonesia

Corresponding Author Email: aulaalansari@gmail.com

https://doi.org/10.18280/rcma.360419

Received: 13 June 2026
Revised: 11 August 2026
Accepted: 20 August 2026
Available online: 31 August 2026

Keywords:
waste glass powder, natural sand replacement, sustainable concrete, mechanical performance, water absorption, chloride-rich exposure, Scanning Electron Microscopy/Energy-Dispersive X-ray Spectroscopy, visual corrosion assessment

ABSTRACT

This study investigated fine waste glass powder (WGP), obtained from clear soda-lime beverage glass and passing the No. 200 sieve, as a partial replacement for natural sand in concrete. Five mixtures containing 0%, 5%, 10%, 15%, and 20% WGP by mass of fine aggregate (FA) were prepared at a constant water/cement ratio of 0.45. Mechanical properties were evaluated through compressive, flexural, and splitting tensile strength tests under 28- and 56-day water curing and after 28 days of immersion in a 35 g/L sodium chloride (NaCl) solution following 28 days of water curing. Water absorption, localized Scanning Electron Microscopy (SEM)/Energy-Dispersive X-ray Spectroscopy (EDS) observations, and qualitative visual examination of embedded steel after 28 accelerated wetting-drying cycles were also conducted. Three specimens were tested for each mechanical and absorption condition, and results were analysed using one-way analysis of variance (ANOVA) and Tukey's honestly significant difference (HSD) test. WGP10 achieved the highest compressive strengths of 45.90, 48.16, and 46.99 MPa, splitting tensile strengths of 2.70, 3.15, and 2.91 MPa, and flexural strengths of 3.46, 3.59, and 3.52 MPa. Water absorption decreased from 5.18% for WGP0 to 3.88% for WGP10. Overall, 10% WGP showed the most favourable performance, while a higher replacement ratio reduced performance. The results indicate short-term property retention but do not establish long-term chloride resistance.

1. INTRODUCTION

Reinforced concrete structures exposed to marine and chloride-rich environments are vulnerable to progressive deterioration due to the penetration and accumulation of chloride ions through the concrete cover. When the chloride concentration at the steel-concrete interface reaches a critical level, the protective passive layer surrounding the reinforcing steel may be disrupted, initiating localized corrosion. The accumulation of corrosion products can generate internal tensile stresses, promote cracking and cover deterioration, weaken the bond between concrete and reinforcement, and eventually reduce the service life of reinforced concrete structures [1]. Chloride transport is affected by several factors, including pore connectivity, internal moisture, temperature, exposure duration, concrete quality, and the availability of water and oxygen. Laboratory chloride exposure is commonly simulated using either continuous immersion or repeated Wetting/Drying (W/D) cycles. Continuous immersion represents a highly saturated chloride-rich condition, whereas W/D exposure combines capillary absorption during wetting with evaporation and salt accumulation during drying [2, 3]. The duration of the wetting and drying phases and the exposure temperature can significantly influence chloride movement and accumulation [4, 5]. Accelerated W/D conditioning at elevated temperature can therefore shorten laboratory exposure periods, but the resulting conditions are more severe than typical field exposure and should be interpreted as comparative laboratory conditions rather than direct predictions of long-term marine performance [4].

The construction industry is also under increasing pressure to reduce the consumption of natural aggregates and to make greater use of recycled materials. Natural sand is widely consumed as fine aggregate (FA), while excessive extraction can contribute to riverbed degradation, groundwater disturbance, and depletion of natural resources [6]. WG represents a potential alternative because it is widely available, non-biodegradable, and can be processed by washing, crushing, grinding, and sieving for use in concrete. Partial replacement of natural sand with recycled glass may therefore reduce both glass disposal and the demand for virgin FA [7].

The performance of concrete containing recycled glass, however, cannot be defined by the replacement ratio alone. Glass source and composition, particle size and shape, replacement basis, aggregate grading, Water-to-Cement Ratio (W/C), curing period, compaction, and the property being

evaluated can all influence the measured response. A review by Hasan et al. [8] showed that the favourable glass replacement level varies considerably among published studies, with reported values ranging widely depending on whether glass is used as a replacement for cement or sand and on the test conditions considered. Experimental studies also show this variation. Tamanna et al. [9] reported that moderate recycled Glass Sand (GS) replacement improved compressive strength, whereas higher replacement reduced it. Hadi et al. [10] found favourable mechanical performance at an intermediate waste glass powder (WGP) content used as FA replacement, while Muhedin and Ibrahim [11] showed that the response differed when WGP was used to replace cement compared with natural sand. Dadouch et al. [12] similarly found that the replacement level giving the most favourable compressive response did not necessarily provide the same flexural response. These findings indicate that the favourable WGP content depends strongly on the material form and the performance criterion considered.

Particle size is another important factor. Coarser glass particles generally behave more like aggregate particles, whereas finely ground glass may contribute to physical filling between larger particles. However, excessive fine material may disturb aggregate grading, increase the total particle surface area, and increase the sensitivity of the mixture to mixing and compaction [12, 13]. Tong et al. [14] showed that particle size and the combined use of GS and Glass Powder (GP) can significantly influence mechanical and durability-related properties, although their system included both aggregate and binder replacement. Bhat et al. [15] also demonstrated that the favourable replacement level changes depending on whether glass is used as coarse aggregate, FA, or powder. Finely ground glass has additionally been investigated for possible pozzolanic behaviour because of its high silica content. Nevertheless, Scanning Electron Microscopy (SEM) and Energy-Dispersive X-ray Spectroscopy (EDS) observations alone cannot confirm glass dissolution, secondary Calcium Silicate Hydrate (C-S-H) formation, or a pozzolanic reaction. Such conclusions require complementary phase or reaction-based techniques. Therefore, without direct confirmation, improvements in strength or absorption should be discussed mainly in terms of possible physical filling and particle-packing contributions [16].

Recent studies have expanded the assessment of waste glass concrete beyond mechanical strength. Gholampour et al. [17] showed that GS can reduce water absorption even when the corresponding mechanical improvement is limited, confirming that different performance indicators may identify different favourable replacement levels. Son et al. [18] reported improved mechanical and durability-related performance when natural FA was completely replaced with pretreated GS, although this system differs from the use of untreated WGP as a partial sand replacement. Studies that directly examined chloride transport have also reported beneficial effects under particular material systems. Wang et al. [19] quantified chloride diffusion in WG concrete under combined carbonation and chloride exposure, while Zhang et al. [20] reported improvements in local microstructure and chloride-related behaviour when GP was used as a cement replacement in seawater-mixed steel-fibre mortar. These studies provide useful chloride-related evidence, but their materials and exposure conditions differ from conventional concrete containing untreated fine WGP used only as a partial replacement for natural sand.

Kadhim and Muttar [21] also investigated GP concrete under combined chloride and sulfate exposure after an initial water-curing period. However, the exposed specimens were compared with strength values obtained before the additional exposure period rather than with water-cured specimens of the same total age. This is important because concrete can continue to develop strength beyond 28 days. Consequently, when specimens are cured for 28 days and then exposed to an aggressive solution for a further period, comparison only with a 28-day reference may combine the influence of environmental exposure with continued age-related strength development. A detailed comparison of the selected previous studies and their differences from the present work is provided in Supplementary Table S1.

The available literature therefore shows that recycled glass can influence mechanical properties, water absorption, microstructure, and chloride-related behaviour, but the reported favourable replacement level remains highly dependent on the glass form, replacement basis, particle size, treatment method, and exposure condition. Relatively limited information is available from a single experimental programme combining five replacement levels of untreated fine WGP below 75 μm used only as a partial replacement for natural sand, an equal age comparison between water-cured and continuously sodium chloride (NaCl) immersed concrete, water absorption, localized SEM/EDS observations, and qualitative examination of embedded conventional reinforcing steel under a separately defined accelerated chloride W/D regime. In addition, many studies that investigate chloride-related behaviour use cement replacement, pretreated glass, mortar systems, combined chemical exposure, or do not include an age-matched water-cured reference [14, 18-21].

To clarify the differences between the selected studies and to situate the present research within the available literature, Table S1 summarises the form of WG, the replacement programme, the main tests, the numerical results, and their relevance to the scope of the present research.

To reduce the influence of specimen age, the present study included specimens cured in water for 56 days as an age-matched reference for specimens initially cured for 28 days and then continuously immersed in NaCl solution for a further 28 days. Fine untreated WGP obtained from clear soda-lime beverage glass and passing the No. 200 sieve was used to replace 0%, 5%, 10%, 15%, and 20% of natural sand by mass at a constant W/C ratio of 0.45. Compressive, flexural, and splitting tensile strengths were evaluated under water curing and continuous chloride-rich immersion, and the mechanical results were supported by water absorption measurements. Selected WGP0 and WGP10 specimens were further examined using SEM and EDS under water curing and accelerated chloride W/D exposure, while embedded conventional steel bars were evaluated qualitatively after the same accelerated W/D conditioning.

The present work therefore focuses on the combined evaluation of mechanical performance, water absorption, localized microstructural and elemental observations, and qualitative visible reinforcement condition while maintaining a clear distinction between continuous NaCl immersion used for mechanical specimens and accelerated W/D conditioning used for SEM/EDS and embedded steel observations. SEM/EDS results are interpreted only as localized supporting evidence and are not used to confirm pozzolanic activity, quantitative pore refinement, or specific crystalline phases.

Similarly, the visual steel assessment is not interpreted as a quantitative corrosion-rate measurement. The study does not propose a universal optimum WGP replacement level; rather, it identifies the replacement level showing the most favourable combined observed performance within the specific materials, mixture proportions, curing ages, and laboratory exposure conditions investigated.

2. MATERIALS AND METHODS

All the experimental configurations were conducted in the Laboratory of Civil Engineering faculty belonging to the Universiti Tenaga Nasional (UNITEN), Malaysia, where an investigation was performed within the usage of WGP as a partial replacement for the original and natural sand in concrete under normal water curing and chloride-rich laboratory exposure. Five mixtures containing 0%, 5%, 10%, 15%, and 20% WGP by mass of total FA were included and prepared, and the experimental program included the compressive, flexural, and splitting tensile strengths in addition to the water absorption, SEM/EDS analysis, and qualitative visual assessment of embedded steel reinforcement.

2.1 Constituent materials

Ordinary Portland Cement (OPC) conforming to ASTM C150/C150M Type I [22] was used as the binder in all concrete mixtures. Natural sand conforming to ASTM C33/C33M [23] was used as the FA. Before mixing, the natural sand was oven-dried at 100 ℃ for 24 h to obtain an oven-dry condition and minimize variations associated with aggregate moisture.

Crushed limestone was used as the coarse aggregate. The coarse-aggregate particle size ranged from 4.75 to 20 mm and complied with the grading requirements of ASTM C33/C33M [23]. Clean tap water obtained from the UNITEN laboratory was used for mixing, curing, and preparation of the chloride-rich solution.

Table 1. Summary of the constituent materials

Material	Description and Specification
Cement	Ordinary Portland Cement (OPC), ASTM C150/C150M Type I [22]
Fine aggregate (FA)	Natural sand conforming to ASTM C33/C33M [23]
Fine aggregate (FA) condition	Oven-dried at 100 ℃ for 24 h
Coarse aggregate	Crushed limestone conforming to ASTM C33/C33M [23]
Coarse aggregate size	4.75-20 mm
Waste glass	Clear soda-lime beverage glass
WGP preparation	Washing, drying, crushing, grinding, and sieving
WGP size classification	Passing the No. 200 sieve
Mixing and curing water	Clean laboratory tap water
Chloride solution	35 g/L NaCl, approximately 3.5% w/v
Reinforcing steel	Steel bar with a nominal diameter of 10 mm

Note: Waste glass powder (WGP), sodium chloride (NaCl).

The WG used in this study was obtained from discarded clear soda lime beverage glass bottles. The bottles were well washed to remove labels, dust, and other organic residues. The clean glass was dried under laboratory conditions, then crushed into smaller parts, mechanically ground, and powdered, and subsequently sieved in accordance with ASTM C136/C136M [24]. Only the particles passing through sieve No. 200 were used in the concrete mixes.

A NaCl solution was prepared by dissolving 35 g of NaCl in 1 L of water, equal to a concentration of 35 g/L, equivalent to around 3.5% w/v. The solution was used as a simplified chloride-rich laboratory exposure medium and was not intended to reproduce the complete chemical composition of natural or synthetic seawater.

Steel reinforcing bars with a nominal diameter of 10 mm were embedded in selected concrete cube specimens for qualitative visual assessment of corrosion after accelerated chloride W/D conditioning. A summary of the constituent materials is provided in Table 1.

2.2 Particle-size distribution of waste glass powder

The particle-size distribution of the WGP was determined using laser diffraction particle size analysis in accordance with ISO 13320 [25]. The analysis was performed using a device at UNITEN University with wet dispersion. For wet dispersion, water was used. The optical model, refractive index settings, and dispersion conditions were selected according to the instrument operating procedure.

Three repeated measurements were conducted using representative samples obtained from the same WGP batch used in the concrete mixtures. The particle size distribution was expressed on a volume basis. The characteristic diametersD_{10}, D_{50} and D_{90} represent the particle sizes below which 10%, 50%, and 90% of the measured particle volume occurred, respectively.

The distribution span was calculated using Eq. (1):

$$Span = \frac{D_{90} - D_{10}}{D_{50}} \quad (1)$$

The repeated particle-size measurements are presented in Table 2.

Table 2. Repeated laser particle-size measurements of waste glass powder (WGP)

Measurement	D_{10}, µm	D_{50}, µm	D_{90}, µm	Span
Run 1	3.70	19.20	65.80	3.23
Run 2	3.90	19.80	66.70	3.17
Run 3	3.80	19.70	66.40	3.18
Mean	3.80	19.57	66.30	3.19
Standard deviation (SD)	0.10	0.32	0.46	0.03

The mean D_{10}, D_{50}, and D_{90} values were 3.80, 19.57, and 66.30 µm, respectively. The low standard deviations (SDs) indicated limited variation among the three measurements. The D_{90} result showed that 90% of the measured particle volume was finer than approximately 66.30 µm, which was consistent with the preparation procedure in which only WGP passing through the No. 200 sieve was retained.

The calculated mean span was 3.19, indicating a relatively broad particle size distribution within the fraction finer than 75 µm. The cumulative volume-based particle size distribution is presented in Table 3 and Figure 1.

The measured distribution confirmed that the WGP contained both very fine particles and particles approaching the upper No. 200 sieve limit. This distribution was consistent with a possible physical filling contribution within the concrete matrix. However, particle size analysis was not, on its own, considered direct evidence of an increase in pore volume or pozzolanic activity.

Table 3. Cumulative volume-based particle-size distribution of waste glass powder (WGP)

Particle Size, μm	Cumulative Volume Undersize, %
1.0	1
2.0	4
3.0	7
3.8	10
5.0	14
10.0	28
15.0	40
19.6	50
25.0	57
30.0	63
40.0	72
50.0	81
55.0	85
60.0	88
66.3	90
70.0	95
75.0	100

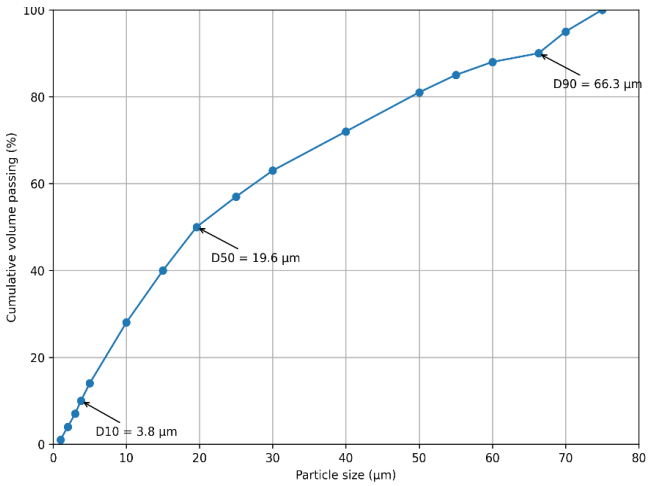

Figure 1. Cumulative volume-based particle-size distribution of the waste glass powder (WGP) determined by laser diffraction

2.3 Mix proportions and mixture design

The proportions of the reference concrete mix were determined to achieve a target 28-day cube compressive strength of approximately 35 MPa, using a nominal W/C ratio of 0.45. The quantities listed in Table 4 represent a single batch of laboratory mixes. The reference batch consists of 25 kg of OPC, 11.2 liters of mixing water, 43 kg of natural sand, and 65 kg of coarse aggregate made from crushed limestone, as shown in Table 4. The calculated W/C ratio was 0.448, whilst the nominal ratio was recorded as 0.45, using standard ASTM C192/C192M-26 [26].

WGP was used as a partial replacement for natural sand on an equal-mass basis at replacement levels of 0%, 5%, 10%, 15%, and 20% of the total FA mass. The mixtures were designated WGP0, WGP5, WGP10, WGP15, and WGP20, respectively.

The cement content, mixing water quantity, coarse aggregate content, and total FA mass were maintained constant for all mixtures. The total FA mass was fixed at 43 kg per laboratory batch, while the quantities of natural sand and WGP were adjusted according to the selected replacement level, as presented in Table 5. No volumetric correction was applied because the replacement procedure was defined on a mass basis.

The same mixture proportions were used for all curing ages and exposure conditions, including the 28 and 56 days water cured specimens, the NaCl-immersed specimens, the water absorption specimens, the specimens selected for SEM/EDS analysis, and the reinforced specimens used for qualitative visual corrosion assessment.

Table 4. Concrete mix proportions and design criteria

Material	Quantity
OPC cement	25 kg
Water	11.2 L
Natural sand	43 kg
Coarse aggregate	65 kg
W/C ratio	0.45
Target strength	≈ C35

Note: Ordinary Portland Cement (OPC).

Table 5. Mix proportions of concrete containing different waste glass powder (WGP) replacement ratios

Mix ID	WGP Replacement, %	Natural Sand, kg	WGP, kg
WGP0	0	43.00	0.00
WGP5	5	40.85	2.15
WGP10	10	38.70	4.30
WGP15	15	36.55	6.45
WGP20	20	34.40	8.60

2.4 Specimen preparation

Concrete specimens were prepared for mechanical testing, water absorption, SEM/EDS analysis, and qualitative visual assessment of embedded steel. For each mixture and mechanical testing condition, three specimens were prepared and tested. Cube specimens measuring 100 × 100 × 100 mm were used for compressive strength, prisms measuring 100 × 100 × 500 mm for flexural strength, and cylinders measuring 150 mm in diameter and 300 mm in height for splitting tensile strength. Additional cubes, prisms, and cylinders were prepared for 56-day water curing to provide age-matched reference specimens for the corresponding NaCl-exposed specimens. Three cubes were also prepared for water absorption for each mixture, giving a total of 15 specimens.

Reinforced concrete cubes containing 10 mm diameter steel bars were prepared for qualitative corrosion observation. SEM/EDS analysis was limited to WGP0 and WGP10, with two localized regions examined for each selected mixture and exposure condition. The dry materials were first mixed, followed by gradual addition of water until a uniform mixture was obtained. The concrete was placed in the moulds in three layers and compacted to reduce air entrapment. After 24 h under laboratory conditions, the specimens were demoulded and transferred to clean water until the required curing age or exposure condition. Specimen preparation and conditioning followed ASTM C192/C192M [26].

2.5 Curing and chloride exposure conditions

After demoulding, the specimens were cured in clean water until the required testing or exposure age. Mechanical specimens were tested after 28 and 56 days of water curing. Separate specimens were initially water-cured for 28 days and then continuously immersed in a 35 g/L NaCl solution, approximately 3.5% w/v, for a further 28 days. These specimens were therefore tested at a total age of 56 days and were compared mainly with the corresponding 56-day water-cured specimens to reduce the influence of specimen age.

For SEM/EDS analysis and qualitative visual assessment of embedded steel, selected specimens were water-cured for 28 days and then subjected to 28 accelerated W/D cycles. Each 24 h cycle consisted of 12 h immersion in the same 35 g/L NaCl solution followed by 12 h oven drying at 60 ℃.

Accordingly, two chloride-exposure regimes were used: continuous NaCl immersion for mechanical testing and accelerated W/D exposure for SEM/EDS and visual corrosion assessment. Because the 60 ℃ drying condition represents a severe accelerated laboratory exposure, the W/D results were interpreted as comparative laboratory observations rather than direct predictions of long-term field performance.

2.6 Mechanical testing methods

Mechanical tests were conducted to evaluate the effect of fine WGP replacement on the strength performance of concrete under normal water curing and chloride-rich exposure. The testing program included cube compressive strength, flexural strength of prism specimens, and splitting tensile strength of cylindrical specimens. For each mixture and testing condition, three specimens were tested, and the results were reported as the mean value, SD, and coefficient of variation (COV).

The specimens assigned to normal curing were continuously cured in clean water for either 28 or 56 days. The NaCl-exposed specimens were initially cured in clean water for 28 days and then continuously immersed in a 35 g/L NaCl solution, equivalent to approximately 3.5% w/v, for an additional 28 days, resulting in a total specimen age of 56 days. Therefore, the mechanical properties of the NaCl-exposed specimens were mainly compared with those of the corresponding 56-day water-cured specimens to minimize the influence of specimen age on the interpretation of the exposure effect.

Cube compressive strength was determined using 100 × 100 × 100 mm cube specimens. The compressive strength was calculated by dividing the maximum applied load by the loaded cross-sectional area of the cube specimen, using standard BS EN 12390 [27], as expressed in Eq. (2):

$$f_c = \frac{P}{A} \tag{2}$$

where, f_c is the cube compressive strength in MPa, P is the maximum applied load in N, and A is the loaded area in mm². For the100 × 100 mm loaded face, the loaded area was 10,000 mm².

Flexural strength was determined using 100 × 100 × 500 mm concrete prism specimens subjected to center-point loading with reference to ASTM C293/C293M [28]. Each specimen was positioned symmetrically on two supporting rollers, and a single concentrated load was applied at the midpoint of the support span until failure.

The modulus of rupture was calculated using Eq. (3):

$$R = \frac{3PL}{2bd^2} \tag{3}$$

where, R is the modulus of rupture in MPa, P is the maximum applied load in N, L is the support span measured between the centers of the supporting rollers in mm, b is the average specimen width in mm, and d is the average specimen depth in mm.

Splitting tensile strength was determined using cylindrical specimens with a diameter of 150 mm and a length of 300 mm in accordance with ASTM C496/C496M [29]. The splitting tensile strength was calculated using Eq. (4):

$$f_t = \frac{2P}{\pi LD} \tag{4}$$

where, f_t is the splitting tensile strength in MPa, P is the maximum applied load in N, L is the cylinder length in mm, and D is the cylinder diameter in mm.

The mechanical test results were statistically analyzed using one-way analysis of variance (ANOVA) to evaluate the effect of WGP replacement level on each measured mechanical property. The analysis was conducted separately for each curing age and exposure condition to avoid combining the effects of specimen age and chloride exposure.

When ANOVA indicated a statistically significant difference among the mixture means, Tukey's honestly significant difference (HSD) post-hoc test was applied to identify significant differences between individual mixtures. Statistical significance was evaluated at a significance level of $\alpha = 0.05$, where $p < 0.05$ indicated a statistically significant difference.

The one-way ANOVA evaluated the effect of WGP replacement level within each individual curing or exposure condition. Therefore, differences between the 56-day water-cured specimens and the corresponding NaCl-exposed specimens were interpreted as numerical exposure-related changes unless a separate statistical comparison between the two exposure conditions was conducted.

2.7 Water absorption test

Water absorption was determined in accordance with BS 1881-122:2011 + A1:2020 [30]. Three concrete cube specimens measuring 100 × 100 × 100 mm were tested for each WGP replacement level, giving a total of 15 specimens.

Before testing, the specimens were oven-dried at 105 ± 5 ℃ until a constant mass was achieved. The specimens were initially dried for approximately 24 h and, where necessary, drying was continued until successive mass measurements indicated that a constant dry mass had been reached. After drying, the specimens were removed from the oven and allowed to cool to room temperature in a desiccator or dry environment for approximately 30-60 min. The oven-dry mass of each specimen, W_d, was then recorded.

The dried specimens were subsequently completely immersed in clean water maintained at approximately 20 ± 2 ℃ for 24 h. At the end of the immersion period, the specimens were removed from the water, and excess surface water was carefully removed using a damp cloth without extracting water from the internal pores. The specimens were

then weighed immediately to determine the saturated mass, W_s.

The water absorption was calculated using Eq. (5):

$$WA(\%) = \frac{W_s - W_d}{W_d} \times 100 \quad (5)$$

where, WA is the water absorption expressed as a percentage, W_d is the oven-dry mass of the specimen in grams, and W_s is the saturated mass after water immersion in grams.

For each mixture, the water absorption result was reported as the mean of three specimens together with the SD and COV. The test was used to provide an indirect indication of accessible pore-related water uptake. It was not interpreted as a direct measurement of total porosity, chloride diffusion, chloride migration, or chloride penetration depth.

2.8 Scanning Electron Microscopy and Energy-Dispersive X-ray Spectroscopy analysis

SEM and EDS analyses were conducted to examine the localized microstructural morphology and elemental composition of selected concrete mixtures. The analyses were performed on WGP0 and WGP10 specimens. WGP0 represented the reference mixture, whereas WGP10 was selected because it exhibited the most favourable overall mechanical and water-absorption performance within the investigated replacement range. Accordingly, the SEM/EDS investigation was intended to provide a localized comparison between the reference and selected WGP-containing mixtures rather than a complete quantitative microstructural assessment of all replacement levels.

For each selected mixture, samples were obtained from specimens subjected to normal water curing and accelerated chloride W/D exposure. The chloride-exposed specimens were initially cured in clean water for 28 days and subsequently subjected to 28 W/D cycles. Each cycle consisted of 12 h of immersion in a solution of 35 g of NaCl per litre of water, corresponding approximately to 3.5% w/v, 60 ℃, followed by 12 h of oven drying at 60 ℃.

Small concrete fragments were collected from internal regions of the specimens and prepared for SEM observation. Two localized regions were examined for each selected mixture and exposure condition. The SEM observations were focused on the characteristic differences in matrix morphology, visible pores, microcracks, crystalline deposits, and the interfaces between the paste and aggregates. Because only a limited number of localized regions were examined, the observations were not considered representative of the entire concrete matrix.

EDS analyses were performed on selected local areas to identify the principal detected elements, including oxygen, silicon, calcium, sodium, aluminium, magnesium, potassium, iron, and other elements present within the analyzed regions. The EDS results were interpreted as localized and semi-quantitative elemental information rather than as representative bulk chemical compositions of the concrete specimens.

The SEM and EDS observations were used only as supporting evidence when discussing the mechanical-strength and water-absorption trends. These analyses were not considered sufficient to confirm pozzolanic activity, identify crystalline phases definitively, quantify total porosity, measure pore-size distribution, or establish quantitative interfacial-transition-zone refinement.

2.9 Visual corrosion observation of embedded steel

Reinforced concrete specimens containing embedded steel bars with a nominal diameter of 10 mm were prepared to qualitatively assess the visible corrosion condition of the reinforcement after accelerated chloride exposure. Following demoulding, the specimens were initially cured in clean water for 28 days and were subsequently subjected to 28 accelerated chloride W/D cycles.

Each cycle consisted of 12 h of complete immersion in a NaCl solution prepared by dissolving 35 g of NaCl in 1 L of water, corresponding to a concentration of 35 g/L or approximately 3.5% w/v, followed by 12 h of oven drying at 60 ℃. One complete W/D cycle therefore lasted 24 h, and the total accelerated exposure period was 28 days.

After completion of the exposure period, the concrete specimens were carefully broken to expose and extract the embedded steel bars. Care was taken during extraction to avoid additional mechanical damage to the steel surfaces. The bars extracted from similar directions were photographed, and the visual inspection focused on the sections that had been embedded within the concrete.

The qualitative assessment took into account the colour, distribution, continuity and approximate longitudinal extent of the visible corrosion products. Reddish-brown or dark-brown surface deposits were considered evidence of visible corrosion, whereas areas retaining a comparatively clean or dark-grey steel surface were considered to exhibit limited visible corrosion. Corrosion occurring on protruding or externally exposed portions of the bars was not considered representative of the protective performance of the surrounding concrete.

Because the assessment was based exclusively on visual inspection, the observations were used only to compare the relative visible corrosion tendency among the investigated mixtures. No half-cell potential, corrosion-current density, electrochemical impedance, or gravimetric mass-loss measurements were conducted. Therefore, the results were not interpreted as quantitative measurements of corrosion rate, corrosion penetration, or steel cross-sectional loss.

3. RESULTS AND DISCUSSION

3.1 Cube compressive strength

The cube compressive strength results under normal water curing and continuous NaCl immersion are presented in Tables 6, S2, and Figure 2. Three specimens were tested for each mixture and condition, and the results were expressed as the mean, SD, and COV. The SD values ranged from 0.32 to 0.50 MPa and the COV values from approximately 1.03% to 1.05%, indicating limited specimen to specimen variation and good repeatability.

One-way ANOVA showed that the WGP replacement level had a statistically significant effect on compressive strength under 28 days water curing, $F(4, 10) = 623.26$, $p < 0.001$; 56-day water curing, $F(4, 10) = 566.39$, $p < 0.001$; and NaCl exposure at a total age of 56 days, $F(4, 10) = 590.70$, $p < 0.001$. Tukey's HSD test showed that WGP10 had significantly higher compressive strength than WGP0, WGP5, WGP15, and WGP20 under all three conditions, while WGP5

was also significantly higher than WGP0. At 28 days, WGP0 and WGP15 were not significantly different (p = 0.124), whereas WGP15 became significantly lower than WGP0 after 56-day water curing (p= 0.010) and NaCl immersion (p = 0.012).

Table 6. Statistical summary and one-way analysis of variance (ANOVA) results for compressive strength

Mix ID	WGP Replacement, %	28-Day Water Mean ± SD, MPa	COV, %	56-Day Water Mean ± SD, MPa	COV, %	NaCl 56-Day Mean ± SD, MPa	COV, %
WGP0	0	35.14 ± 0.37^{c}	1.05	37.03 ± 0.39^{c}	1.05	36.10 ± 0.37^{c}	1.04
WGP5	5	37.35 ± 0.39^{b}	1.05	40.15 ± 0.42^{b}	1.04	38.42 ± 0.40^{b}	1.05
WGP10	10	45.90 ± 0.48^{a}	1.04	48.16 ± 0.50^{a}	1.05	46.99 ± 0.49^{a}	1.04
WGP15	15	34.29 ± 0.36^{c}	1.04	35.58 ± 0.37^{d}	1.03	34.72 ± 0.36^{d}	1.04
WGP20	20	31.10 ± 0.32^{d}	1.04	33.90 ± 0.35^{e}	1.04	32.61 ± 0.34^{e}	1.04
ANOVA F(4, 10)	—	623.26	—	566.39	—	590.70	—
p-value	—	< 0.001	—	< 0.001	—	< 0.001	—

Note: Values within the same exposure condition sharing the same superscript letter are not significantly different according to Tukey's HSD test at α = 0.05. n = 3 specimens per mixture and condition; waste glass powder (WGP); coefficient of variation (COV); standard deviation (SD); sodium chloride (NaCl).

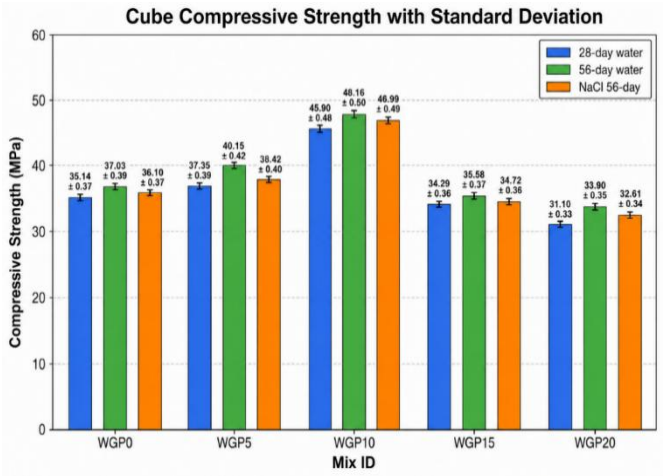

Figure 2. Compressive strength of waste glass powder (WGP) concrete with standard deviation (SD)
Note: Error bars represent ±1 SD; n = 3 specimens per group.

After 28 days of water curing, WGP0 recorded 35.14 MPa. The strength increased to 37.35 MPa for WGP5, corresponding to an increase of approximately 6.3%, and reached the highest value of 45.90 MPa for WGP10, approximately 30.6% above the control. The improvement at moderate WGP replacement may be associated with the fine glass particles occupying some spaces between the paste and aggregate constituents and contributing to more efficient particle packing. However, because pore-size distribution and Interfacial Transition Zone (ITZ) properties were not quantitatively measured, this explanation represents a possible physical contribution rather than direct evidence of pore refinement.

Increasing the WGP replacement level above 10% reduced compressive strength. WGP15 and WGP20 recorded 34.29 and 31.10 MPa, corresponding to reductions of approximately 2.4% and 11.5%, respectively, compared with WGP0 at 28 days. The decline at higher replacement levels may be associated with changes in fine-aggregate gradation, increased particle surface area, and greater sensitivity to mixing and compaction when a larger proportion of natural sand is replaced.

After 56 days of water curing, all mixtures showed higher compressive strength than at 28 days. WGP0, WGP5, WGP10, WGP15, and WGP20 reached 37.03, 40.15, 48.16, 35.58, and 33.90 MPa, respectively. The increase was consistent with continued cement hydration, while WGP10 remained the highest-performing mixture and was approximately 30.1% higher than the corresponding control.

The NaCl-exposed specimens followed the same general replacement-level trend. WGP0, WGP5, WGP10, WGP15, and WGP20 recorded 36.10, 38.42, 46.99, 34.72, and 32.61 MPa, respectively. WGP10 again achieved the highest value and was approximately 30.2% higher than the NaCl-exposed control. Compared with the corresponding 56 days water cured specimens, the NaCl-exposed strengths were numerically lower by approximately 2.5%, 4.3%, 2.4%, 2.4%, and 3.8% for WGP0, WGP5, WGP10, WGP15, and WGP20, respectively. The specimens therefore retained approximately 95.7-97.6% of their corresponding 56 days water-cured compressive strength.

Because the one-way ANOVA was performed separately within each curing or exposure condition, the differences between the 56 days water cured and NaCl-exposed specimens should be interpreted as numerical strength-retention differences rather than statistically confirmed exposure effects. The limited reductions after NaCl immersion may be associated with the penetration of the chloride-rich solution into accessible pores and localized changes within the matrix. However, the exposure period was relatively short and compressive strength is not a direct measure of chloride penetration or migration; therefore, the results should not be considered conclusive evidence of long-term chloride resistance.

Overall, compressive strength increased up to 10% WGP replacement and decreased at 15% and 20%. WGP10 provided the highest compressive strength under all investigated curing and exposure conditions and therefore showed the most favorable compressive-strength performance within the materials and conditions examined in this study.

3.2 Flexural strength of prism specimens

The flexural strength results under water curing and NaCl exposure are presented in Table 7 and Figure 3, while the individual specimen results are provided in Supplementary Table S3. Three specimens were tested for each mixture and condition, and the results were reported as the mean, SD, and COV. The SD values ranged from approximately 0.05 to 0.08 MPa and the COV values from 1.64% to 2.30%, indicating limited variation and acceptable repeatability among the specimens.

One-way ANOVA showed that WGP replacement level had a statistically significant effect on flexural strength under 28-day water curing, $F(4, 10) = 131.07$, $p < 0.001$; 56-day water curing, $F(4, 10) = 99.45$, $p < 0.001$; and NaCl exposure at a total age of 56 days, $F(4, 10) = 112.23$, $p < 0.001$. Tukey's HSD test showed that WGP10 was significantly higher than WGP0, WGP15, and WGP20 under all three conditions. WGP5 and WGP10 were statistically comparable after 28-day water curing and NaCl exposure, whereas WGP10 became significantly higher than WGP5 after 56 days of water curing.

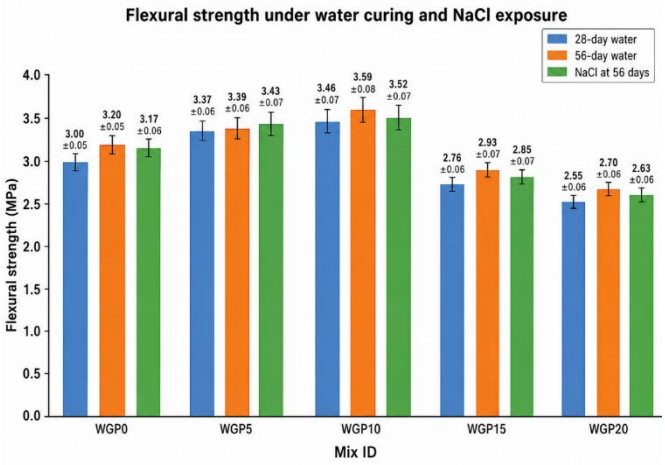

Figure 3. Flexural strength of waste glass powder (WGP) concrete under water curing and sodium chloride (NaCl) exposure with standard deviation (SD)
Note: Error bars represent ±1 SD; n = 3 specimens per group.

After 28 days of water curing, WGP0 recorded a mean flexural strength of 3.00 MPa. WGP5 increased the strength to 3.37 MPa, approximately 12.3% above the control, while WGP10 achieved the highest value of 3.46 MPa, approximately 15.3% higher than WGP0. The improvement at moderate WGP replacement may be associated mainly with the micro-filler effect of the fine glass particles, which may occupy spaces between the cement paste and aggregate particles and contribute to improved particle packing and stress transfer. However, the flexural strength results alone do not prove a pozzolanic reaction, and any chemical contribution should therefore be interpreted cautiously.

Above 10% replacement, flexural strength decreased significantly. WGP15 and WGP20 recorded 2.76 and 2.55 MPa, approximately 8.0% and 15.0% lower than WGP0, respectively. The reduction at higher WGP contents may be associated with excessive fine particles, changes in fine-aggregate gradation, increased sensitivity to particle distribution and compaction, and possible localized agglomeration. These effects may create weak regions that promote crack initiation and propagation during flexural loading.

After 56 days of water curing, WGP0, WGP5, WGP10, WGP15, and WGP20 recorded 3.20, 3.39, 3.59, 2.93, and 2.70 MPa, respectively. WGP10 remained the highest-performing mixture and was approximately 12.2% higher than the corresponding control. Between 28 and 56 days, WGP10 increased by approximately 3.8%, while WGP5 increased by approximately 0.6%. The overall increase was consistent with continued cement hydration and strengthening of the cementitious matrix. At 56 days, Tukey's test confirmed that WGP10 was significantly higher than WGP5.

After NaCl exposure, the same general trend remained. WGP0, WGP5, WGP10, WGP15, and WGP20 recorded 3.17, 3.43, 3.52, 2.85, and 2.63 MPa, respectively. Relative to the NaCl-exposed control, WGP5 and WGP10 were approximately 8.2% and 11.0% higher, whereas WGP15 and WGP20 were approximately 10.1% and 17.0% lower. WGP10 had the highest numerical mean; however, Tukey's test showed no significant difference between WGP5 and WGP10 under NaCl exposure.

Table 7. Statistical summary and one-way analysis of variance (ANOVA) results for flexural strength under different curing and NaCl exposure conditions

Mix ID	WGP, %	28-Day Water, Mean ± SD (MPa)	COV, %	56-Day Water, Mean ± SD (MPa)	COV, %	NaCl at 56 Days, Mean ± SD (MPa)	COV, %
WGP0	0	3.00 ± 0.05^{b}	1.76	3.20 ± 0.05^{c}	1.65	3.17 ± 0.06^{b}	1.76
WGP5	5	3.37 ± 0.06^{a}	1.65	3.39 ± 0.06^{b}	1.64	3.43 ± 0.07^{a}	1.91
WGP10	10	3.46 ± 0.07^{a}	2.08	3.59 ± 0.08^{a}	2.10	3.52 ± 0.07^{a}	1.86
WGP15	15	2.76 ± 0.06^{c}	2.02	2.93 ± 0.07^{d}	2.24	2.85 ± 0.07^{c}	2.30
WGP20	20	2.55 ± 0.06^{d}	2.18	2.70 ± 0.06^{e}	2.06	2.63 ± 0.06^{d}	2.12
ANOVA $F(4, 10)$	—	131.07	—	99.45	—	112.23	—
p-value	—	< 0.001	—	< 0.001	—	< 0.001	—

Note: Values within the same exposure condition sharing the same superscript letter are not significantly different according to Tukey's HSD test at $\alpha = 0.05$. One-way ANOVA indicated a significant effect of WGP replacement level under all three conditions. n = 3 specimens per mixture and condition. Waste glass powder (WGP), coefficient of variation (COV), standard deviation (SD), sodium chloride (NaCl).

Comparison with the corresponding 56 days water-cured specimens showed only limited numerical changes after NaCl exposure. WGP0, WGP10, WGP15, and WGP20 decreased by approximately 0.9%, 1.9%, 2.7%, and 2.6%, respectively. WGP5 showed a slight increase from 3.39 to 3.43 MPa, equivalent to approximately 1.2%; however, the difference was only 0.04 MPa and was consistent with the SD of the measurements. Therefore, this increase should be considered minor experimental variation rather than evidence that NaCl exposure improved flexural strength.

The slight reductions observed after NaCl immersion may be associated with the penetration of the chloride-rich solution into accessible pores and localized changes within the cementitious matrix. However, the exposure period was limited to 28 days after initial water curing, and the observed changes were small. These mechanisms should therefore be interpreted cautiously and not as evidence of widespread chloride-induced deterioration. In addition, because the ANOVA was conducted separately within each curing or exposure condition, the differences between the 56-day water-

cured and NaCl-exposed specimens represent numerical strength-retention changes rather than statistically confirmed exposure effects.

Overall, flexural strength increased up to 10% WGP replacement and decreased at 15% and 20%. WGP10 achieved the highest mean flexural strength under all investigated conditions, although WGP5 and WGP10 were statistically comparable after 28 days of water curing and NaCl exposure. Therefore, WGP10 showed the most favorable overall flexural strength performance within the investigated materials, replacement levels, curing ages, and exposure conditions.

3.3 Splitting tensile strength of cylindrical specimens

The splitting tensile strength results under water curing and continuous NaCl immersion are presented in Table 8 and Figure 4, while the individual specimen results are provided in Supplementary Table S4. Three cylindrical specimens were tested for each mixture and condition, and the results were reported as the mean, SD, and COV. The SD values ranged from approximately 0.05 to 0.07 MPa and the COV values from 1.98% to 2.65%, indicating limited variation and acceptable repeatability.

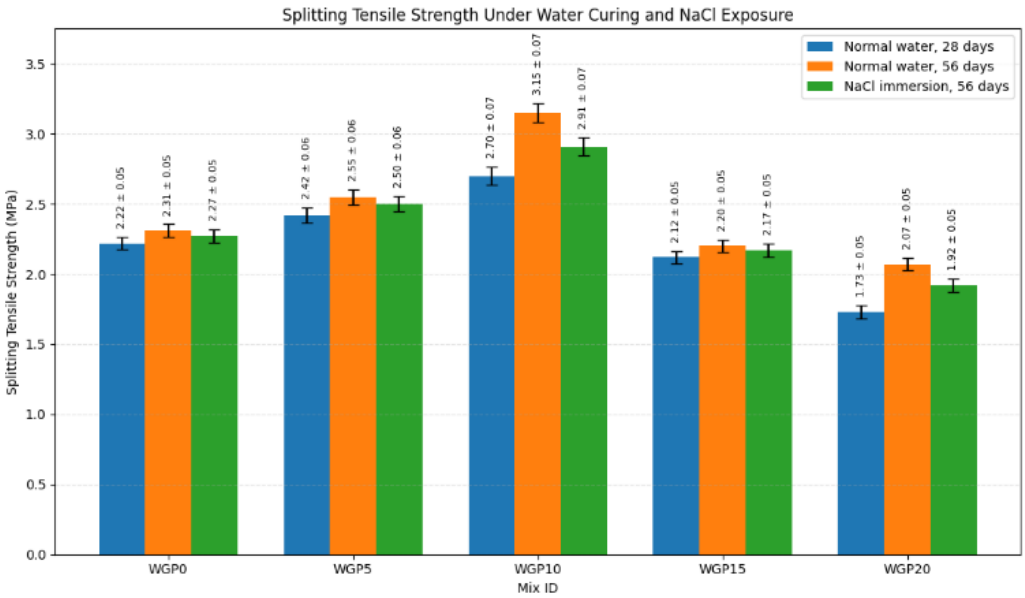

Figure 4. Splitting tensile strength of waste glass powder (WGP) concrete under water curing and sodium chloride (NaCl) exposure with standard deviation (SD)
Note: Error bars represent ±1 SD; n = 3 specimens per group.

Table 8. Statistical summary and one-way analysis of variance (ANOVA) results for splitting tensile strength under different curing and sodium chloride (NaCl) exposure conditions

Mix ID	WGP, %	28-Day Water, Mean ± SD (MPa)	COV, %	56-Day Water, Mean ± SD (MPa)	COV, %	NaCl at 56 Days, Mean ± SD (MPa)	COV, %
WGP0	0	2.22 ± 0.05^{c}	2.06	2.31 ± 0.05^{c}	1.98	2.27 ± 0.05^{c}	2.02
WGP5	5	2.42 ± 0.06^{b}	2.30	2.55 ± 0.06^{b}	2.18	2.50 ± 0.06^{b}	2.23
WGP10	10	2.70 ± 0.07^{a}	2.43	3.15 ± 0.07^{a}	2.08	2.91 ± 0.07^{a}	2.25
WGP15	15	2.12 ± 0.05^{cd}	2.16	2.20 ± 0.05^{cd}	2.08	2.17 ± 0.05^{cd}	2.11
WGP20	20	1.73 ± 0.05^{d}	2.65	2.07 ± 0.05^{d}	2.21	1.92 ± 0.05^{d}	2.39
ANOVA $F(4, 10)$	—	142.03	—	198.81	—	153.21	—
p-value	—	< 0.001	—	< 0.001	—	< 0.001	—

Note: Values within the same curing or exposure condition sharing the same superscript letter are not significantly different according to Tukey's HSD test at α = 0.05. One-way ANOVA indicated a significant effect of WGP replacement level under all three conditions. n = 3 specimens per mixture and condition. Waste glass powder (WGP), coefficient of variation (COV), standard deviation (SD).

One-way ANOVA showed that WGP replacement level had a statistically significant effect on splitting tensile strength under 28 days water curing, $F(4, 10) = 142.03$, $p < 0.001$; 56-day water curing, $F(4, 10) = 198.81$, $p < 0.001$; and NaCl exposure at a total age of 56 days, $F(4, 10) = 153.21$, $p < 0.001$. Tukey's HSD test showed that WGP10 had significantly higher splitting tensile strength than all other mixtures under each condition, while WGP5 was also significantly higher than WGP0, WGP15, and WGP20. At 28 days and after NaCl exposure, WGP0 and WGP15 were statistically comparable. At 56 days, WGP0 and WGP15 were statistically comparable, while WGP15 and WGP20 were also not significantly different.

Under 28-day water curing, WGP0 recorded a mean splitting tensile strength of 2.22 MPa. WGP5 increased the strength to 2.42 MPa, approximately 9.0% above the control, while WGP10 achieved the highest value of 2.70 MPa, approximately 21.6% higher than WGP0. The improvement at moderate WGP replacement may be associated with the fine glass particles occupying some spaces between the cement paste and aggregate constituents and contributing to more efficient particle packing and stress transfer. However, these

results alone do not confirm pore refinement, ITZ improvement, or pozzolanic activity.

Increasing the WGP replacement level above 10% reduced splitting tensile strength. WGP15 and WGP20 recorded 2.12 and 1.73 MPa, approximately 4.5% and 22.1% lower than WGP0, respectively. The reduction at higher replacement levels may be associated with changes in FA gradation, increased particle surface area, greater sensitivity to particle distribution and compaction, and possible localized agglomeration. These effects may create preferred locations for crack initiation during splitting failure.

After 56 days of water curing, WGP0, WGP5, WGP10, WGP15, and WGP20 recorded 2.31, 2.55, 3.15, 2.20, and 2.07 MPa, respectively. The increase with curing age was consistent with continued cement hydration and strengthening of the cementitious matrix. WGP10 increased by approximately 16.7% from its 28-day value and remained the highest-performing mixture, with a splitting tensile strength approximately 36.4% higher than WGP0. Although WGP15 and WGP20 also gained strength, they remained approximately 4.8% and 10.4% below the corresponding control.

Following continuous immersion in the 35 g/L NaCl solution, WGP0, WGP5, WGP10, WGP15, and WGP20 recorded 2.27, 2.50, 2.91, 2.17, and 1.92 MPa, respectively. Relative to the NaCl-exposed control, WGP5 and WGP10 were approximately 10.1% and 28.2% higher, whereas WGP15 and WGP20 were approximately 4.4% and 15.4% lower. WGP10 remained significantly higher than all other mixtures, while no significant difference was observed between WGP0 and WGP15.

Compared with the corresponding 56-day water-cured specimens, splitting tensile strength decreased by approximately 1.7%, 2.0%, 7.6%, 1.4%, and 7.2% for WGP0, WGP5, WGP10, WGP15, and WGP20, respectively. The mixtures therefore retained approximately 92.4-98.6% of their corresponding 56 days water cured strength. WGP15 showed the highest numerical strength retention, while WGP10 maintained the highest absolute splitting tensile strength despite its larger percentage reduction.

The larger reductions observed for WGP10 and WGP20 suggest that the response to NaCl immersion was not controlled only by the initial strength level. Accessible pores, particle arrangement, and localized tensile defects may also have influenced the response, although these factors were not measured quantitatively. The reductions may be associated with the entry of the chloride-rich solution into accessible pores and localized changes within the hardened matrix. However, the exposure period was limited to 28 days after initial water curing, and the splitting tensile test does not directly measure chloride penetration, diffusion, or reinforcement corrosion.

Because the one-way ANOVA was conducted separately within each curing age and exposure condition, the differences between the 56 days water cured and NaCl-exposed specimens should be interpreted as numerical strength retention changes rather than statistically confirmed exposure effects.

Overall, splitting tensile strength increased up to 10% WGP replacement and decreased at 15% and 20%. WGP10 achieved the highest mean splitting tensile strength and was significantly higher than all other mixtures under each investigated condition. Therefore, 10% WGP provided the most favorable splitting tensile strength performance within the materials, replacement levels, curing ages, and exposure conditions examined in this study.

3.4 Water absorption

The water absorption results are presented in Table 9 and Figure 5, while the individual specimen results are provided in Supplementary Table S5. Three specimens were tested for each mixture. The SD values ranged from approximately 0.04% to 0.08%, while the COV values ranged from 0.81% to 2.00%, indicating limited variation and good repeatability.

One-way ANOVA showed that the WGP replacement level had a statistically significant effect on water absorption, $F(4, 10) = 198.54$, $p < 0.001$. Tukey's test showed that WGP10 had significantly lower water absorption than all other mixtures. WGP15 was also significantly lower than WGP0, WGP5, and WGP20, while WGP5 was significantly lower than WGP0 and WGP20. No significant difference was observed between WGP0 and WGP20.

Table 9. Statistical summary and one-way analysis of variance (ANOVA) results for water absorption of waste glass powder (WGP) concrete

Mix ID	WGP Replacement, %	Water Absorption, Mean ± SD, %	COV, %
WGP0	0	5.18 ± 0.06^{d}	1.15
WGP5	5	4.80 ± 0.07^{c}	1.54
WGP10	10	3.88 ± 0.08^{a}	2.00
WGP15	15	4.62 ± 0.04^{b}	0.81
WGP20	20	5.11 ± 0.06^{d}	1.26
ANOVA $F(4,10)$	—	198.54	—
p-value	—	< 0.001	—

Note: Values sharing the same superscript letter are not significantly different according to Tukey's HSD test at $\alpha = 0.05$. One-way ANOVA indicated a significant effect of WGP replacement level on water absorption, $F(4,10) = 198.54$, $p < 0.001$. n = 3 specimens per mixture. Coefficient of variation (COV), standard deviation (SD).

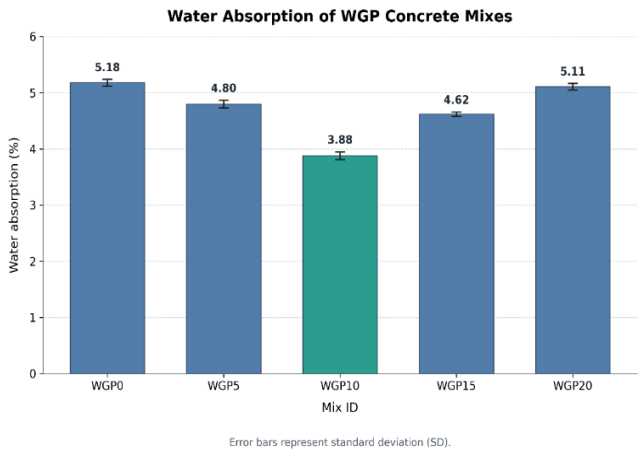

Figure 5. Effect of waste glass powder (WGP) replacement level on water absorption of concrete mixtures
Note: Error bars represent ±1 SD; n = 3 specimens per group.

Water absorption decreased from 5.18% for WGP0 to 4.80% for WGP5, representing a reduction of approximately 7.3%. WGP10 recorded the lowest value of 3.88%, approximately 25.1% lower than WGP0. The lower absorption at moderate WGP replacement may be associated with a possible physical filling contribution from the fine glass particles, which may improve particle packing and reduce

accessible pathways for water uptake. However, water absorption alone does not directly determine total porosity, pore-size distribution, or ITZ properties.

When the WGP replacement level exceeded 10%, water absorption increased. WGP15 recorded 4.62%, approximately 19.1% higher than WGP10 but still 10.8% lower than WGP0. WGP20 recorded 5.11%, approximately 31.7% higher than WGP10 and only 1.3% lower than WGP0. The increase at higher replacement levels may be associated with changes in fine-aggregate grading, increased particle surface area, greater sensitivity to particle dispersion and compaction, and possible localized agglomeration or incomplete compaction.

The water absorption trend was consistent with the mechanical results, as WGP10 combined the lowest water absorption with the highest compressive, flexural, and splitting tensile strengths. This relationship is consistent with a possible improvement in local particle packing at the 10% replacement level, although the internal pore structure was not quantitatively measured.

The water absorption test should therefore be interpreted only as an indirect indicator of accessible pore-related water uptake. The lower absorption of WGP10 does not provide direct evidence of improved chloride resistance, which would require direct chloride migration, diffusion, electrical resistivity, or chloride-profile measurements.

Overall, water absorption decreased up to 10% WGP replacement and increased at 15% and 20%. Within the investigated replacement levels, WGP10 provided the most favorable water absorption performance.

3.5 Microstructural analysis using Scanning Electron Microscopy

SEM was used to examine the local microstructure of WGP0 and WGP10 under normal water curing and NaCl exposure. WGP0 represented the reference concrete without GP, while WGP10 was selected because it exhibited the highest average mechanical strengths and the lowest water absorption within the investigated replacement range. The comparison focused on matrix continuity, visible voids, particle arrangement, surface discontinuities, and exposure-related crystalline deposits.

SEM images were obtained from selected fields at magnifications ranging approximately from ×100 to ×1500. The observations were used to examine the general morphology and local features of the fractured surfaces. These observations are qualitative and do not provide quantitative measurements of total porosity, pore-size distribution, aggregate distribution, or ITZ thickness.

3.5.1 Waste glass powder 0 under normal water curing

SEM images of WGP0 under normal water curing showed a heterogeneous fractured surface containing relatively compact regions together with rougher and more open areas. Irregular cavities, dark voids, granular features, and non-uniform particle contacts were visible within the examined fields. Fine lamellar features and rounded inclusions were also observed locally, with some openings occurring along their boundaries, as shown in Figure 6 and Figure S1.

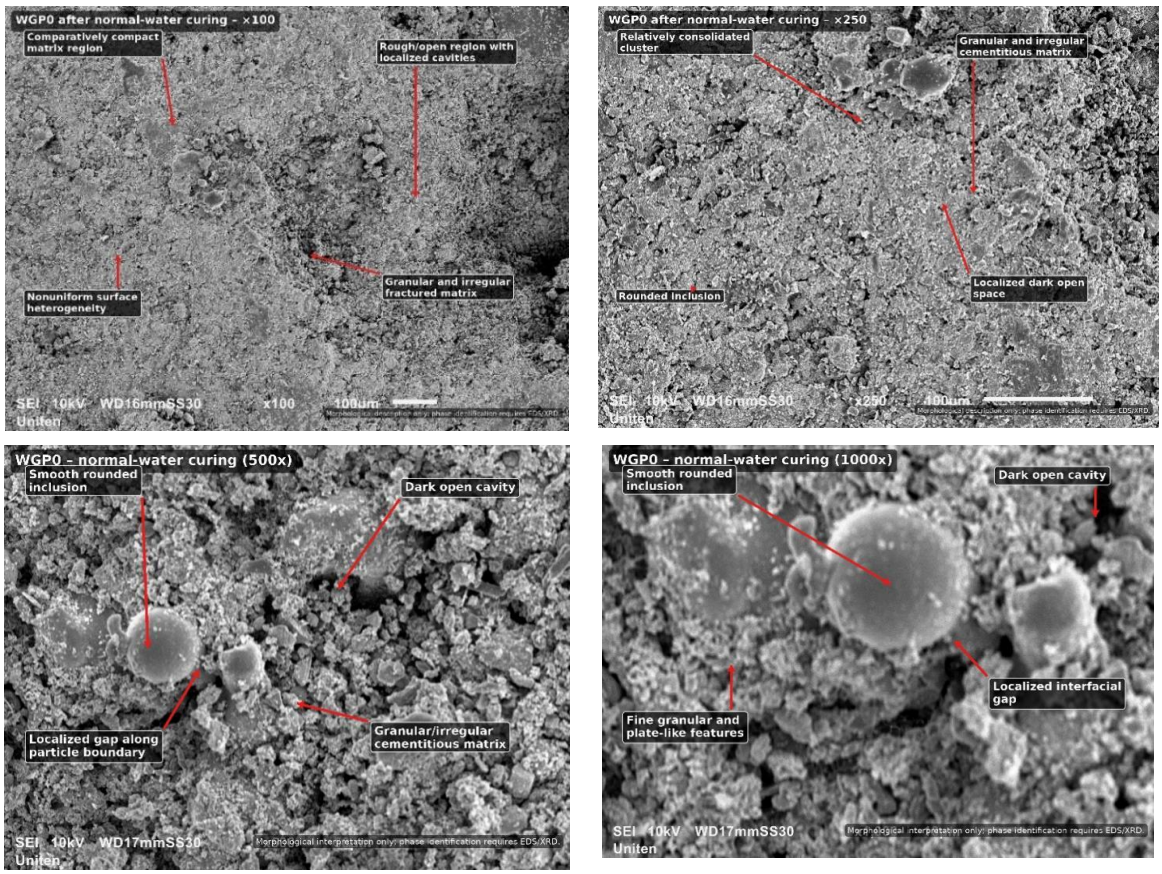

Figure 6. Scanning Electron Microscopy (SEM) micrographs of waste glass powder 0 (WGP0) after normal water curing showing a heterogeneous granular matrix, localized open cavities, and nonuniform particle contacts

No widespread crystalline aggregation or continuous cracking was observed across the examined areas. Localized voids and narrow surface discontinuities remained visible, although some may have been influenced by specimen fracturing and preparation. Overall, WGP0 showed local heterogeneity and variation between relatively compact and

open regions. The SEM images do not permit quantitative measurement of the interfaces or identification of the chemical composition of the observed features.

3.5.2 WGP0 after sodium chloride exposure

After NaCl exposure, WGP0 retained a heterogeneous fractured morphology but showed additional localized surface deposits and crystalline features. Numerous elongated, needle-like, rod-like, and plate-like formations were observed within cavities and along rough regions of the matrix. These features occurred as isolated crystals, bundles, and localized clusters, as shown in Figure 7 and Figure S2.

Open spaces remained visible between many of the deposits, indicating that they did not form a completely continuous or compact layer. No large-scale continuous cracking was observed, although localized gaps and cavities remained around some deposits. The increased occurrence of crystalline features indicates that the chloride-rich W/D exposure was associated with localized precipitation or crystallization. However, their chemical or mineralogical identity cannot be determined from SEM morphology alone; therefore, they are described only as exposure-related crystalline deposits.

3.5.3 Waste glass powder 10 under normal water curing

The water-cured WGP10 sample exhibited a finer and comparatively more continuous local morphology than WGP0. Large irregular openings were less pronounced in several examined areas, while fine particles appeared to occupy spaces between larger constituents and provide more uniform local particle contacts. Some rough areas, small voids, and discontinuities nevertheless remained visible, as shown in Figure 8 and Figure S3.

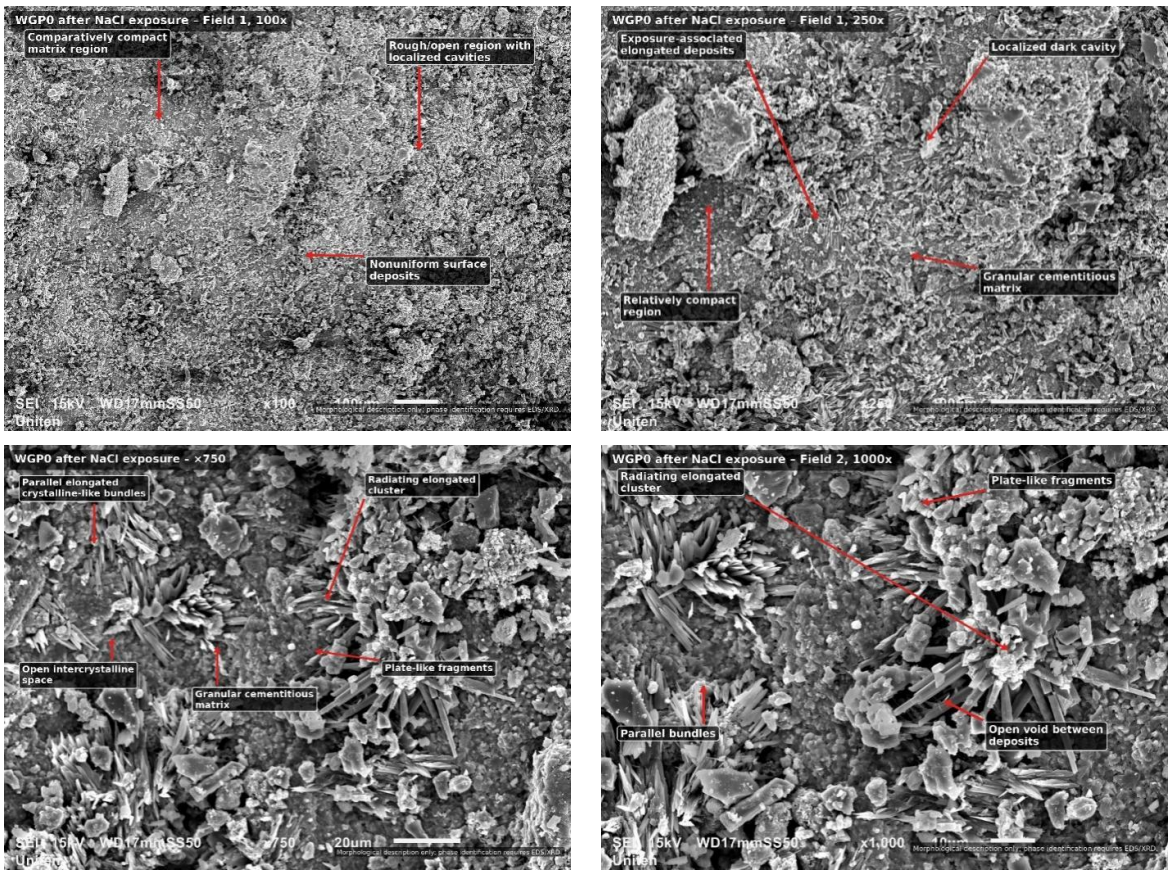

Figure 7. Scanning Electron Microscopy (SEM) micrographs of waste glass powder 0 (WGP0) after sodium chloride (NaCl) exposure showing localized cavities and abundant needle-like, rod-like, and plate-like crystalline deposits

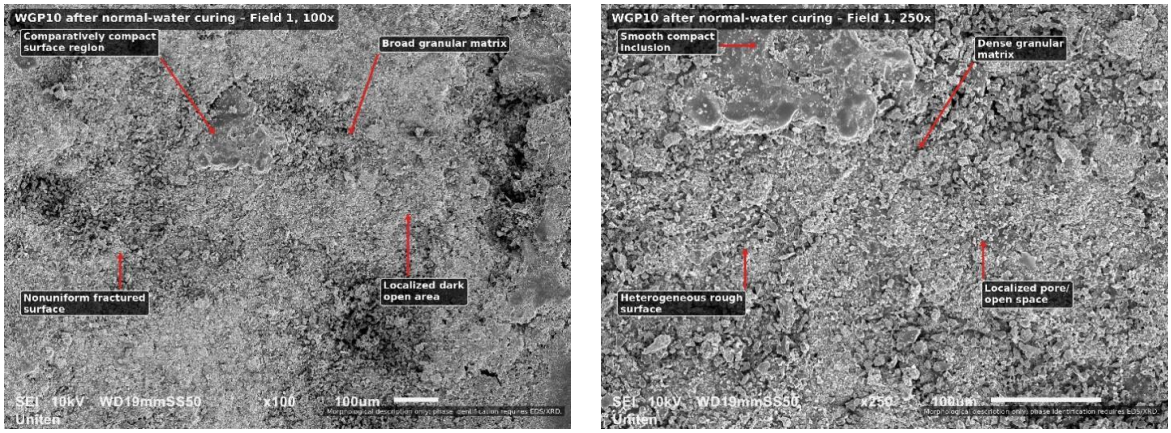

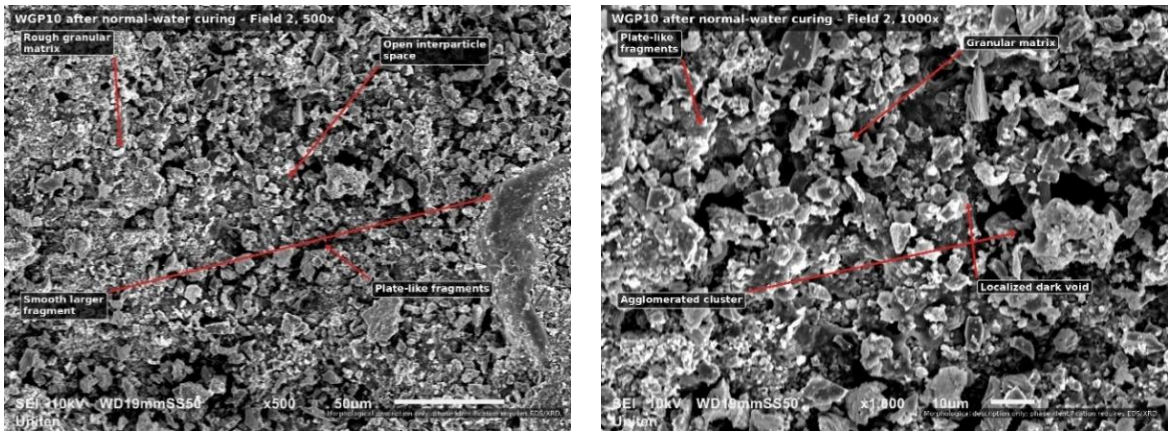

Figure 8. Scanning Electron Microscopy (SEM) micrographs of waste glass powder 10 (WGP10) after normal water curing showing a comparatively continuous matrix, finer particle distribution, and localized interparticle openings

The comparatively more continuous appearance of WGP10 is consistent with a possible physical filling and improved local particle-arrangement contribution from the fine WGP particles, which were smaller than 75 μm. This interpretation is also consistent with the lower water absorption and higher mechanical strength measured for WGP10. However, the SEM observations do not quantitatively confirm pore refinement, ITZ improvement, additional C-S-H formation, or a secondary pozzolanic reaction.

3.5.4 Waste glass powder 10 after sodium chloride exposure

After NaCl exposure, WGP10 showed a clear change in local morphology compared with the water-cured sample. Long prismatic and rod-like crystalline formations were widely observed, together with localized finer needle-like and plate-like deposits. Their distribution was irregular, with crystal-rich areas occurring alongside regions where the granular matrix remained visible, as shown in Figure 9.

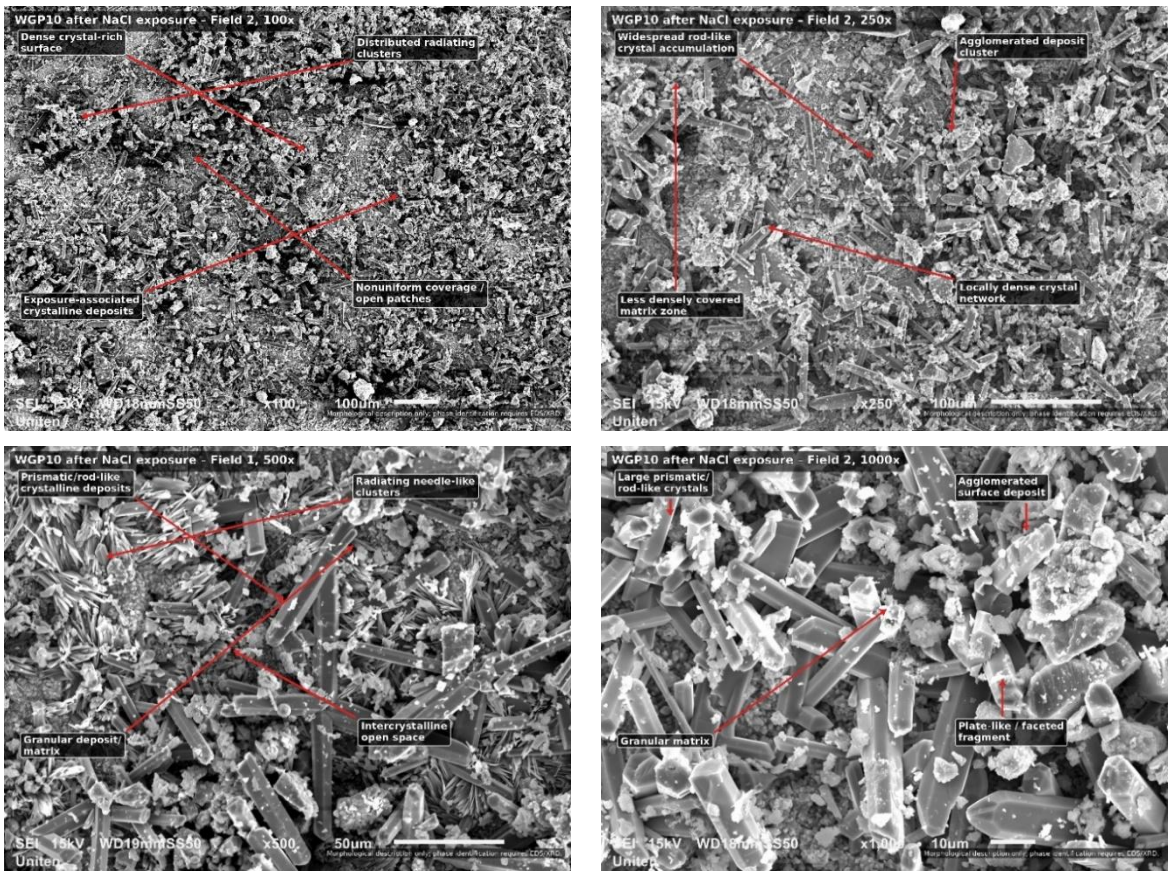

Figure 9. Scanning Electron Microscopy (SEM) micrographs of waste glass powder 10 (WGP10) after sodium chloride (NaCl) exposure showing abundant elongated prismatic and rod-like formations, localized acicular clusters, and intercrystallite spaces

Open voids and discontinuities remained around some deposits, indicating that the crystalline formations did not produce a completely continuous layer. Compared with water-cured WGP10, the exposed sample showed a greater abundance of elongated crystalline features, while cohesive granular regions remained visible and no continuous fracture extended across the examined areas, as shown in Figure S4. These observations indicate localized morphological changes following NaCl exposure but do not establish the chemical identity of the deposits. Therefore, the prismatic, rod-like, and

acicular formations should be described as exposure-related crystalline deposits rather than identified as NaCl or specific chloride-bearing hydration phases.

3.5.5 Comparative microstructural assessment

Comparison of the water-cured mixtures showed that WGP0 contained more pronounced local voids, greater variation between compact and open regions, and less continuous particle contacts. In contrast, WGP10 exhibited a finer and comparatively more continuous local morphology with fewer prominent openings. These observations are consistent with a possible physical filling and improved local particle-arrangement contribution at the 10% WGP replacement level.

After NaCl exposure, both mixtures showed clear morphological changes. WGP0 contained mainly acicular, lamellar, and irregular crystalline deposits, whereas WGP10 showed a greater presence of prismatic and rod-like formations. The 10% WGP content therefore did not prevent crystallization but was associated with differences in the local morphology and distribution of the exposure-related deposits. Because the SEM images represent selected local areas, they cannot be used to determine which mixture contained a greater total amount of deposited material.

The SEM observations must therefore be interpreted qualitatively. The examined areas are not statistically representative of the entire concrete volume, and total porosity, pore connectivity, pore-size distribution, ITZ characteristics, and chloride penetration depth were not quantified. In addition, the chemical identity of the observed granular, lamellar, acicular, prismatic, and rod-like features cannot be determined from morphology alone. Their local elemental compositions are discussed separately using EDS in Section 3.6.

Overall, the water-cured WGP10 sample showed a comparatively more continuous and closely packed local morphology than WGP0, which was consistent with its higher mechanical strengths and lower water absorption. NaCl exposure produced localized crystalline deposits in both mixtures without widespread continuous cracking in the examined fields. However, these observations do not confirm secondary pozzolanic reactions, specific chloride-bearing phases, or quantitative chloride resistance. Within the investigated conditions, the SEM results therefore provide qualitative support for the more favorable overall performance observed for WGP10.

3.6 Elemental analysis using Energy-Dispersive X-ray Spectroscopy

EDS was used to examine the local elemental composition of selected regions from WGP0 and WGP10 under normal water curing and NaCl exposure. WGP0 represented the reference mixture, while WGP10 was selected because it exhibited the highest average mechanical strengths and the lowest water absorption within the investigated replacement range. The measurements were taken from the selected areas shown in the corresponding SEM images and therefore represent localized, semi-quantitative analyses rather than the bulk chemical composition of the concrete. The complete elemental compositions are provided in Supplementary Table S6, while the main comparative indicators are summarized in Table 10.

Table 10. Selected comparative indicators derived from the local EDS analyses

Specimen	Exposure Condition	Na, wt.%	Si, wt.%	Ca, wt.%	Local Ca/Si Atomic Ratio
WGP0	Normal water	1.00	7.44	35.55	3.35
WGP0	NaCl exposure	13.62	7.94	24.56	2.17
WGP10	Normal water	1.14	16.56	23.66	1.00
WGP10	NaCl exposure	0.86	7.86	32.87	2.93

Note: Waste glass powder (WGP), Energy-Dispersive X-ray Spectroscopy (EDS).

Under normal water curing, the selected WGP0 region contained mainly O, Ca, and Si at 51.61, 35.55, and 7.44 wt.%, respectively, as shown in Figure 10. The corresponding WGP10 region contained 49.25 wt.% O, 23.66 wt.% Ca, and 16.56 wt.% Si. Thus, the localized Si content increased by approximately 122.6% from WGP0 to WGP10, while Ca decreased from 35.55 to 23.66 wt.%. The higher Si content is consistent with the presence of silica-rich WGP in the analyzed region. However, these differences do not independently confirm glass dissolution, additional C-S-H formation, calcium consumption, or a secondary pozzolanic reaction because each analyzed area may contain different proportions of glass particles, cement paste, and aggregate-related constituents.

After NaCl exposure, the most pronounced change in the selected WGP0 region was the increase in Na from 1.00 to 13.62 wt.%, while O remained nearly unchanged at 51.13 wt.%. The exposed region also contained 24.56 wt.% Ca and 7.94 wt.% Si, as shown in Figure 11. This localized Na enrichment is consistent with the accumulation of sodium-containing material during NaCl W/D exposure and may be associated with the crystalline deposits observed by SEM. However, Cl was not detected in the spectrum. Therefore, the deposits cannot be identified as NaCl, Friedel's salt, or any other specific chloride-bearing phase.

For WGP10 after NaCl exposure, the selected region contained 42.99 wt.% O, 32.87 wt.% Ca, 7.86 wt.% Si, and 0.86 wt.% Na, as shown in Figure 12. In contrast to WGP0, Na did not increase after exposure, changing from 1.14 wt.% under normal water curing to 0.86 wt.%. This localized difference should not be interpreted as evidence that WGP10 prevented sodium or chloride penetration because the spectra were obtained from different selected regions. Cl was also not detected in the exposed WGP10 spectrum; therefore, the prismatic and rod-like deposits observed by SEM cannot be assigned to a specific chloride-bearing phase.

The WGP10 NaCl spectrum also reported 11.57 wt.% Zr and 2.22 wt.% I, together with smaller amounts of Al, S, and K. Zr and I were not consistently detected in the other analyzed regions, and the EDS report listed the calibration standard for iodine as "not defined." These isolated detections were therefore interpreted cautiously and were not used to establish a chemical reaction mechanism.

The calculated Ca/Si atomic ratio decreased from approximately 3.35 in water-cured WGP0 to 1.00 in water-cured WGP10, mainly because of the higher Si content in the

selected WGP10 region. After NaCl exposure, the corresponding ratios were approximately 2.17 for WGP0 and 2.93 for WGP10. These values are area-averaged ratios from regions containing different particles and phases and should not be interpreted as stoichiometric Ca/Si ratios of C-S-H or as direct evidence of pozzolanic reaction or phase transformation.

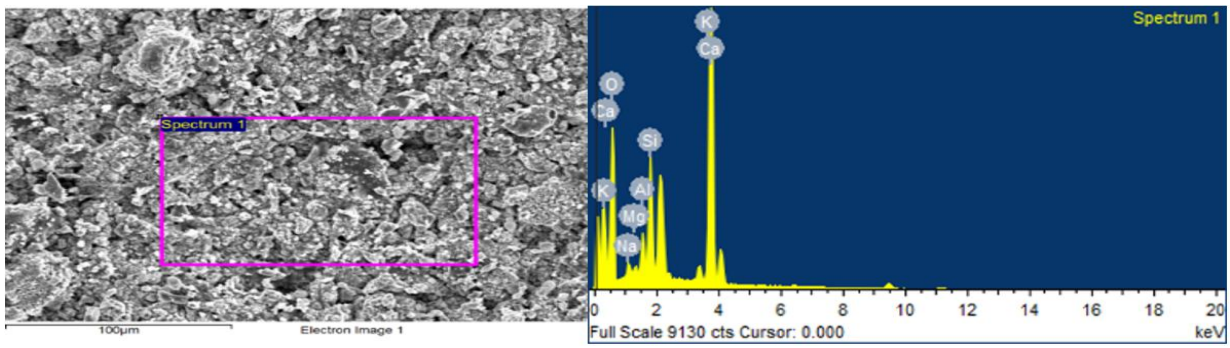

Figure 10. Energy-Dispersive X-ray Spectroscopy (EDS) spectrum and selected analysis area of waste glass powder 0 (WGP0) under normal water

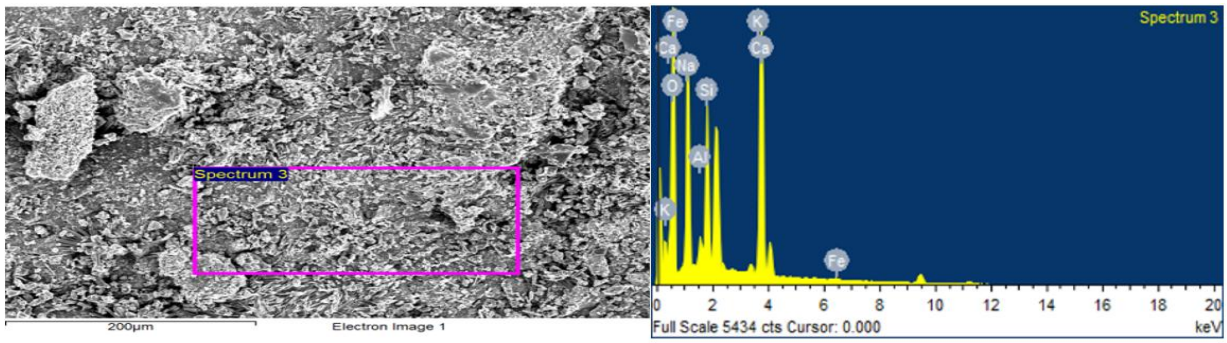

Figure 11. Energy-Dispersive X-ray Spectroscopy (EDS) and selected analysis area for waste glass powder 0 (WGP0) following exposure to sodium chloride (NaCl)

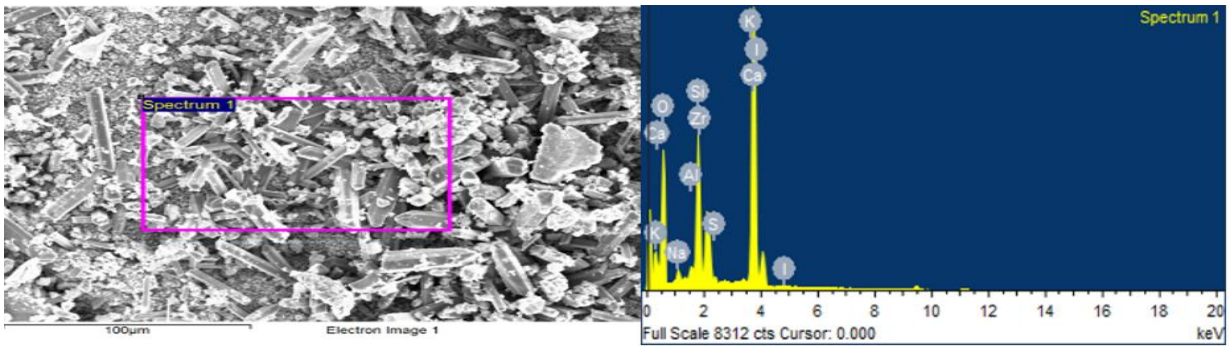

Figure 12. Energy-Dispersive X-ray Spectroscopy (EDS) and selected analysis area for waste glass powder 10 (WGP10) following exposure to sodium chloride (NaCl)

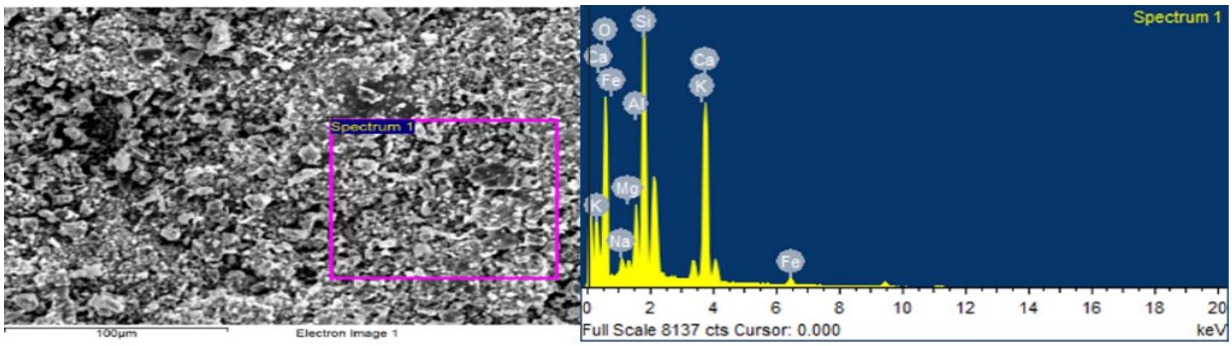

Figure 13. Energy-Dispersive X-ray Spectroscopy (EDS) spectrum and selected analysis area of waste glass powder 10 (WGP10) under normal water

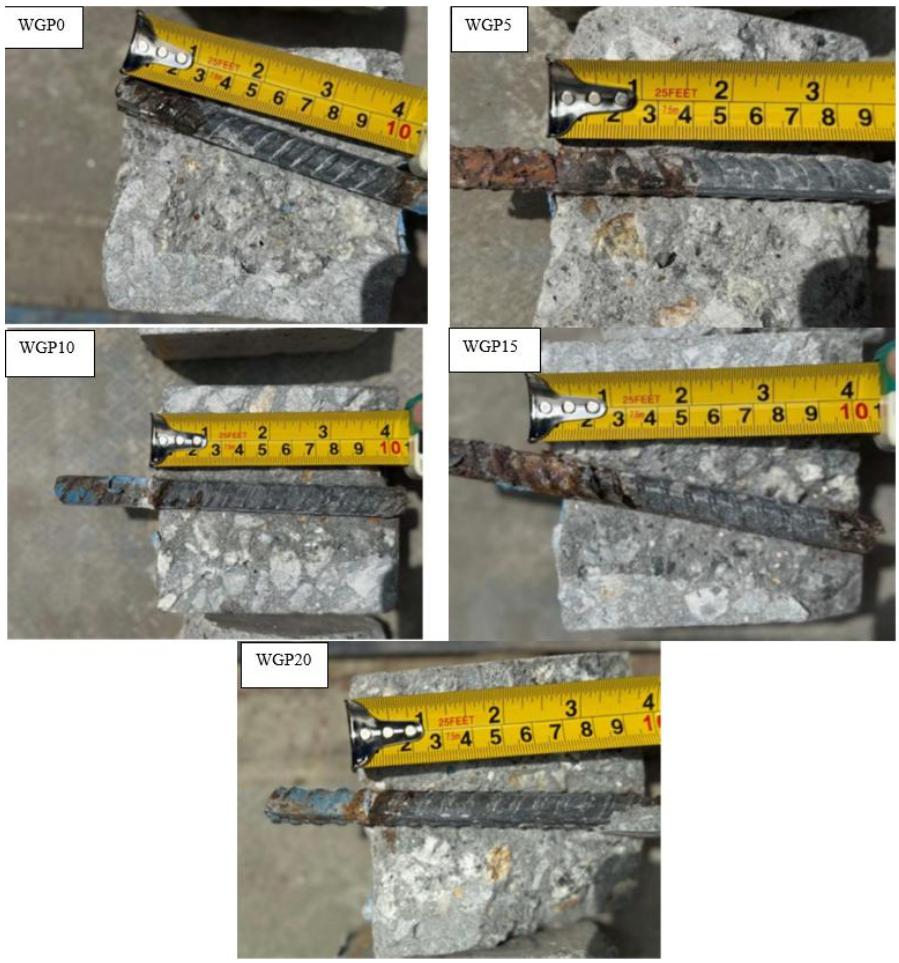

Figure 14. Representative visual condition of embedded steel bars extracted from WGP0, WGP5, WGP10, WGP15, and WGP20 specimens after 28 accelerated NaCl W/D cycles

Note: Waste glass powder (WGP), sodium chloride (NaCl). The observations are qualitative and do not represent corrosion-rate measurements.

The EDS results therefore showed clear local differences between the mixtures and exposure conditions. Water-cured WGP10 exhibited a higher localized Si content, as shown in Figure 13, while the selected NaCl-exposed WGP0 region showed pronounced Na enrichment. However, these differences mainly demonstrate spatial variation in local elemental composition and cannot be used to quantify chloride penetration or salt uptake.

Overall, the EDS results support the SEM observations by showing localized changes in elemental composition following WGP incorporation and NaCl exposure. However, the analyses were localized and semi-quantitative, and Cl was not detected in either exposed spectrum. Therefore, the chemical identity of the crystalline deposits remains undetermined, and the results do not confirm specific hydration phases, secondary pozzolanic reactions, or overall chloride resistance.

3.7 Qualitative visual observation of embedded steel

After completing the chloride exposure testing program, selected concrete specimens were carefully broken to expose and extract the embedded reinforcing steel. During removal, care was taken to avoid any further mechanical damage to the surface of the steel that might affect the later visual assessment. The extracted bars have been placed alongside a measuring tape and photographed from different angles to provide a consistent visual reference for comparing the location and apparent extent of visible corrosion products. The testing focused on the part of each bar that had been previously embedded in the concrete, whilst corrosion showing on the protruding or externally exposed parts was not considered representative of the protective performance of the surrounding concrete.

The visual assessment covered the colour, distribution, continuity, and apparent surface coverage of the corrosion products visible along the length of the integrated reinforcement bar. Areas showing brownish or dark brown deposits were considered to be visually affected by corrosion, whilst the parts retaining a relatively clean ribbed steel surface or a dark grey surface were considered to show limited visible corrosion. The photos showed that the corrosion was not evenly spread across the length of the bars being tested. Instead, visible rust was concentrated in specific areas, whilst the adjacent sections of the same bars remained relatively less affected. In some cases, the corrosion products appeared as isolated surface patches, whereas other areas showed more continuous deposits extending across several adjacent ribs. Variations in the apparent thickness and colour intensity of the rust layers were also observed, indicating differences in the visible surface condition along the examined bars, as shown in Figure 14.

Visual inspection suggested differences in the distribution and apparent surface coverage of corrosion products among the examined reinforcing bars; however, no quantitative ranking of corrosion performance was established from the

photographs. The localized distribution of the visible corrosion products may be associated with differences in the accessibility of chloride-bearing solution, moisture, and oxygen to the steel surface through the surrounding concrete. Local variations in concrete porosity, cracking, interfacial condition, or cover quality may also have influenced the distribution of the visible corrosion products. However, these mechanisms cannot be confirmed from the photographs alone. The visual observations were therefore used only to compare the general surface condition and spatial distribution of visible corrosion products among the examined bars rather than to determine corrosion rate or steel section loss. Because no gravimetric mass-loss measurements or electrochemical tests were conducted, the results represent a qualitative comparison of visible reinforcement deterioration under the investigated extraction and observation conditions.

4. CONCLUSIONS

This study investigated the use of fine, untreated WGP as a partial substitute for natural sand at replacement rates of 0%, 5%, 10%, 15% and 20%. The performance of the mixtures was evaluated through compressive strength, flexural strength, split tensile strength, and water absorption tests, as well as in-situ analysis using a SEM/EDS, and qualitative visual assessment of the embedded steel under hydro-curing conditions and laboratory exposure to a chloride-rich environment. Based on the materials studied, mix proportions, curing periods, and exposure conditions, the following conclusions were reached:

(1) The WGP replacement ratio had a statistically significant effect on compressive, flexural and tensile strength under all the curing and exposure conditions studied. The mechanical response was non-linear, with performance generally improving up to a WGP replacement level of 10%, before declining at 15% and 20%. This confirms that increasing the WGP content beyond a moderate replacement level did not provide any additional mechanical benefit.

(2) Material WGP10 exhibited the best overall mechanical performance. Its compressive strength was 45.90, 48.16, and 46.99 MPa after 28 days of water curing, 56 days of water curing, and exposure to a NaCl solution, respectively. The corresponding flexural strengths were 3.46, 3.59, and 3.52 MPa, while the splitting tensile strengths were 2.70, 3.15, and 2.91 MPa. WGP10 was significantly stronger than the other mixtures in compressive and splitting tensile strength, although WGP5 and WGP10 were statistically comparable in flexural strength under 28 days of water curing and NaCl exposure.

(3) The inclusion of 56-day water-cured specimens provided an equal-age reference for the NaCl-exposed specimens and reduced the confounding effect of continued curing. Relative to the corresponding 56-day water-cured specimens, the NaCl-exposed mixtures generally showed only limited numerical reductions in compressive and flexural strengths, whereas splitting tensile strength showed greater sensitivity in some mixtures, particularly WGP10 and WGP20. These differences represent numerical strength-retention changes because the statistical analyses were conducted separately within each curing or exposure condition.

(4) Water absorption decreased from 5.18% for WGP0 to a minimum of 3.88% for WGP10, corresponding to a reduction of approximately 25.1%. Absorption subsequently increased to 4.62% and 5.11% for WGP15 and WGP20, respectively. The combination of lower water absorption and higher mechanical strength observed for WGP10 is consistent with a possible physical filling and improved particle-packing contribution of the fine glass particles, although total porosity, pore connectivity, and ITZ characteristics were not quantitatively measured.

(5) Localized SEM observations showed that the selected water-cured WGP10 regions exhibited a comparatively more continuous and closely arranged morphology than the corresponding WGP0 regions. Following accelerated NaCl W/D exposure, both mixtures developed localized crystalline deposits with different morphologies. These observations were qualitative and limited to selected fractured surfaces and therefore cannot be interpreted as quantitative measurements of pore refinement, deposited material, or bulk microstructural change.

(6) EDS analysis showed a higher local silicon contribution in the selected water-cured WGP10 region, consistent with the incorporation of silica-rich soda-lime GP. However, the localized and semi-quantitative EDS results did not confirm glass dissolution, additional C-S-H formation, secondary pozzolanic activity, or the chemical identity of the exposure-associated crystalline deposits. The absence of detected chlorine in the exposed spectra also prevented direct identification of chloride-bearing phases.

(7) The embedded steel bars exhibited localized and nonuniform visible corrosion products after accelerated W/D exposure. These observations were used only to compare the general surface condition of the examined reinforcement. Because electrochemical measurements and gravimetric mass-loss testing were not conducted, the results do not provide quantitative information on corrosion rate, corrosion penetration, or steel section loss.

(8) Within the specific WGP source, particle-size range, mixture proportions, curing ages, and laboratory exposure conditions investigated, WGP10 provided the most favorable combined mechanical and water absorption performance. This result should not be interpreted as a universal optimum for all WG concrete, because the favorable replacement level may vary with glass composition, particle-size distribution, replacement basis, W/C ratio, curing regime, and the performance criterion considered.

Limitations and future work: This study is limited to short term mechanical performance, water absorption, local observations using an SEM/EDS, and a visual assessment of the strength of the matrix under standard laboratory exposure conditions. The results should therefore not be taken as direct proof of long-term chloride resistance or of the quantitative performance of the reinforcement in terms of corrosion resistance. Future investigation should include tests for chloride migration or direct diffusion, electrical resistivity, chloride concentration profiles, quantitative characterisation of the pore structure, X-ray Diffraction (XRD) or Thermogravimetric Analysis (TGA), and electrochemical or gravimetric corrosion measurements.

ACKNOWLEDGMENT

The authors express their appreciation to the Higher Institution Centre of Excellence (HICoE), Ministry of Higher Education (MOHE), Malaysia, for their support under Project

Code 2024001HICOE, as referenced in JPT(BPKI)1000/016/018/34(5). The authors would also like to acknowledge the support of UNITEN and the Civil Engineering Laboratory for providing essential facilities, technical assistance, and resources that contributed significantly to the successful completion of this work.

REFERENCES

[1] Ali, M., Shams, M.A., Bheel, N., et al. (2024). A review on chloride induced corrosion in reinforced concrete structures: Lab and in situ investigation. RSC Advances, 14(50): 37252-37271. https://doi.org/10.1039/D4RA05506C

[2] Wang, L.B., Zhou, H.J., Lian, S.S., Tang, X.D. (2024). Drying-wetting correlation analysis of chloride transport behavior and mechanism in calcium sulphoaluminate cement concrete. Materials, 17(18): 4600. https://doi.org/10.3390/ma17184600

[3] Ou, Y.L., Xu, M.J., Chen, D.Q., Jiang, M.J., Xiao, L., Mei, G.X. (2022). Effect of reverse water pressure on chloride penetration within finite concrete during drying-wetting cycles. Ocean Engineering, 257: 111606. https://doi.org/10.1016/j.oceaneng.2022.111606

[4] Chen, C.H., Wang, L., Liu, R.G., et al. (2023). Chloride penetration of concrete exposed to dry-wet cycle with various dry-wet ratios and temperature. Construction and Building Materials, 400: 132883. https://doi.org/10.1016/j.conbuildmat.2023.132883

[5] Bao, J.W., Zheng, R., Wei, J.N., Zhang, P., Xue, S.B., Liu, Z.L. (2022). Numerical and experimental investigation of coupled capillary suction and chloride penetration in unsaturated concrete under cyclic drying-wetting condition. Journal of Building Engineering, 51: 104273. https://doi.org/10.1016/j.jobe.2022.104273

[6] Dinh, H.L., Liu, J., Ong, D.E.L., Doh, J.H. (2022). A sustainable solution to excessive river sand mining by utilizing by-products in concrete manufacturing: A state-of-the-art review. Cleaner Materials, 6: 100140. https://doi.org/10.1016/j.clema.2022.100140

[7] Epure, C., Munteanu, C., Istrate, B., Harja, M., Buium, F. (2023). Applications of recycled and crushed glass (RCG) as a substitute for natural materials in various fields-a review. Materials, 16(17): 5957. https://doi.org/10.3390/ma16175957

[8] Hasan, A.A.A.J., Syamsir, A., Woen, E.L., Najeeb, M.I., Anggraini, V. (2025). A review on the effect of chemical and physical properties of glass powder towards the concrete performance. Revue des Composites et des Matériaux Avancés-Journal of Composite and Advanced Materials, 35(3): 543-557. https://doi.org/10.18280/rcma.350315

[9] Tamanna, N., Tuladhar, R., Sivakugan, N. (2020). Performance of recycled waste glass sand as partial replacement of sand in concrete. Construction and Building Materials, 239: 117804. https://doi.org/10.1016/j.conbuildmat.2019.117804

[10] Hadi, R.A., Abd, S.M., Najm, H.M., Qaidi, S., Eldirderi, M.A., Khedher, K.M. (2023). Influence of recycling waste glass as fine aggregate on the concrete properties. Journal of Renewable Materials, 11(6): 2925-2940. https://doi.org/10.32604/jrm.2023.025558

[11] Muhedin, D.A., Ibrahim, R.K. (2023). Effect of waste glass powder as partial replacement of cement & sand in concrete. Case Studies in Construction Materials, 19: e02512. https://doi.org/10.1016/j.cscm.2023.e02512

[12] Dadouch, M., Belal, T., Ghembaza, M.S. (2024). Valorization of glass waste as partial substitution of sand in concrete-investigation of the physical and mechanical properties for a sustainable construction. Construction and Building Materials, 411: 134436. https://doi.org/10.1016/j.conbuildmat.2023.134436

[13] Ishaq, M.B., Mohammed, A.S., Mohammed, A.A. (2025). Influence of waste glass powder particle size gradation on the mechanical properties and workability of sustainable green concrete. Structural Concrete, 26(6): 7752-7776. https://doi.org/10.1002/suco.70237

[14] Tong, G.J., Pang, J.Y., Shen, J.Z., et al. (2024). Response tests on the effects of particle size of waste glass sand and glass powder on the mechanical and durability performance of concrete. Scientific Reports, 14(1): 25445. https://doi.org/10.1038/s41598-024-76164-9

[15] Bhat, K.R., Dumre, G., Gyawali, T.R. (2024). Transforming waste into strength: evaluating properties of concrete with waste glass substitution. Cleaner Waste Systems, 9: 100179. https://doi.org/10.1016/j.clwas.2024.100179

[16] Li, Q., Qiao, H.X., Li, A.Y., Li, G.J. (2022). Performance of waste glass powder as a pozzolanic material in blended cement mortar. Construction and Building Materials, 324: 126531. https://doi.org/10.1016/j.conbuildmat.2022.126531

[17] Gholampour, A., Ozbakkaloglu, T., Valizadeh Kiamahalleh, M., Gencel, O. (2025). Waste glass as a substitution for binder and sand in concrete: mechanical and physical properties. Innovative Infrastructure Solutions, 10(5): 179. https://doi.org/10.1007/s41062-025-02011-z

[18] Son, M., Kim, G., Eu, H., et al. (2025). Effect of pretreated waste glass sand on comprehensive performance of concrete based on mechanical properties, durability, and microstructure. Construction and Building Materials, 487: 141963. https://doi.org/10.1016/j.conbuildmat.2025.141963

[19] Wang, H.Z., Wen, B., Xu, P., Zhang, L., Niu, D.T., Berardi, M. (2025). Study on chloride ion diffusion behavior of waste glass concrete under carbonation and chloride corrosion. Case Studies in Construction Materials, 23: e05309. https://doi.org/10.1016/j.cscm.2025.e05309

[20] Zhang, X.W., Lu, J.X., Poon, C.S. (2025). Enhancing microstructural properties and chloride resistance of seawater-mixed steel fiber-reinforced mortars through glass powder modification. Materials and Structures, 58(4): 143. https://doi.org/10.1617/s11527-025-02669-y

[21] Kadhim, H.J., Muttar, A.A. (2026). Durability performance of concrete incorporating green glass powder as cement replacement under chloride and sulfate attack. Revue des Composites et des Matériaux Avancés-Journal of Composite and Advanced Materials, 36(3): 597-610. https://doi.org/10.18280/rcma.360314

[22] ASTM International. (2024). ASTM C150/C150M-24: Standard specification for portland cement. ASTM International. https://doi.org/10.1520/C0150_C0150M-24

[23] ASTM International. (2024). ASTM C33/C33M-24a: Standard specification for concrete aggregates. ASTM

International. https://doi.org/10.1520/C0033_C0033M-24A
[24] ASTM International. (2025). ASTM C136/C136M-25: Standard test method for sieve analysis of fine and coarse aggregates. ASTM International. https://doi.org/10.1520/C0136_C0136M-25
[25] Organización Internacional de Normalización. (2020). ISO 13320: 2020: Particle size analysis: Laser diffraction methods. ISO.
[26] ASTM International. (2026). ASTM C192/C192M-26: Standard practice for making and curing concrete test specimens in the laboratory. ASTM International. https://doi.org/10.1520/C0192_C0192M-26
[27] British Standards Institution (BSI). (2019). BS EN 12390:2019, Testing hardened concrete-compressive strength of test specimen. British Standards Institution, London, UK. https://doi.org/10.3403/30360097
[28] ASTM International. (2016). ASTM C293/C293M-16: Standard test method for flexural strength of concrete (using simple beam with center-point loading). ASTM International. https://doi.org/10.1520/C0293_C0293M-16
[29] ASTM International. (2017). ASTM C496/C496M-17: Standard test method for splitting tensile strength of cylindrical concrete specimens. ASTM International. https://doi.org/10.1520/C0496_C0496M-17
[30] British Standards Institution. (2020). BS 1881 122: 2011+ A1: 2020. Testing concrete: Part 122. Method for determination of water absorption. British Standards Institution.

NOMENCLATURE

ANOVA	Analysis of Variance
ASTM	ASTM International
BS	British Standard
BSI	British Standards Institution
COV	Coefficient of Variation
C-S-H	Calcium Silicate Hydrate
EDS	Energy-Dispersive X-ray Spectroscopy
FA	Fine Aggregate
GGBS	Ground Granulated Blast-Furnace Slag
GP	Glass Powder
GS	Glass Sand
HICoE	Higher Institution Centre of Excellence
HSD	Honestly Significant Difference
IEI	Institute of Energy Infrastructure
ISO	International Organization for Standardization
ITZ	Interfacial Transition Zone
MOHE	Ministry of Higher Education
NaCl	Sodium Chloride
OPC	Ordinary Portland Cement
SD	Standard Deviation
SEM	Scanning Electron Microscopy
TGA	Thermogravimetric Analysis
UNITEN	Universiti Tenaga Nasional
W/C	Water-to-Cement Ratio
W/D	Wetting/Drying
WG	Waste Glass
WGP	Waste Glass Powder
WGS	Waste Glass Sand
XRD	X-ray Diffraction

Mix and specimen designations

S1	Specimen 1
S2	Specimen 2
S3	Specimen 3
WGP0	Concrete containing 0% WGP replacement
WGP10	Concrete containing 10% WGP replacement
WGP15	Concrete containing 15% WGP replacement
WGP20	Concrete containing 20% WGP replacement
WGP5	Concrete containing 5% WGP replacement

Mathematical and experimental symbols

A	Loaded cross-sectional area
alpha	Statistical significance level
b	Average width of the prism specimen
Ca/Si	Local calcium-to-silicon atomic ratio
d	Average depth of the prism specimen
D	Diameter of the cylindrical specimen
D10	Particle diameter below which 10% of the measured particle volume occurs
D50	Median particle diameter; particle diameter below which 50% of the measured particle volume occurs
D90	Particle diameter below which 90% of the measured particle volume occurs
F	ANOVA F-statistic
fc	Cube compressive strength
ft	Splitting tensile strength
L	Support span in the flexural-strength equation; cylinder length in the splitting-tensile-strength equation
P	Maximum applied load
p	Probability value (p-value)
R	Modulus of rupture / flexural strength
Span	Width of the particle-size distribution, calculated as (D90 - D10) / D50
WA	Water absorption
Wd	Oven-dry mass of the specimen
Ws	Saturated mass of the specimen

Chemical element symbols used in EDS

Al	Aluminium
Ca	Calcium
Cl	Chlorine
Fe	Iron
I	Iodine
K	Potassium
Mg	Magnesium
Na	Sodium
O	Oxygen
S	Sulfur
Si	Silicon
Zr	Zirconium

Units and notations

%	Percent
°C	Degrees Celsius
µm	Micrometre
Avg.	Average
Eq.	Equation
g	Gram

g/L	Grams per litre	N	Newton
h	Hour	No.	Number
ID	Identification	w/v	Weight per volume
kg	Kilogram	wt.%	Weight percent
L	Litre		
mm	Millimetre		
mm²	Square millimetre		
MPa	Megapascal		

SUPPLEMENTARY MATERIAL

Table S1. Demonstrates that the reported favourable glass content varies considerably among studies

Study	WG Application	Replacement Levels	Important Numerical Results	Differences From the Current Study
Hasan et al. [8]	Review of GP as cement or sand replacement	Reported ranges varied among studies	Favourable levels were generally found to be around 20%, but the reported values ranged between 5% and 40%, depending on the size of the glass, the replacement base, the W/C ratio, and the curing time.	Review article; no original chloride-conditioning experiment
Tamanna et al. [9]	Recycled glass sand replacing natural sand	20%, 40%, 60%	20% increased 28-day compressive strength by about 7%; 40% reduced it by about 14%	Coarser recycled glass sand; no integrated SEM/EDS and embedded-steel program
Hadi et al. [10]	Glass powder replacing fine aggregate	15%, 30%, 50%	At 30%, compressive strength increased by 2.4% and 12.45% at 7 and 28 days; tensile strength increased by 2.5% and 26.54%	No chloride conditioning or reinforcement-corrosion assessment
Muhedin and Ibrahim [11]	Glass powder replacing cement and sand separately	5%, 10%, 15%, 20%	Moderate cement replacement of 5–15% improved strength at several ages; higher contents reduced the response, particularly when replacing sand	Included XRD/SEM, but not controlled water-versus-NaCl equal-age comparison
Dadouch et al. [12]	Recycled glass replacing natural sand	10%, 20%, 30%	The 20% mixture retained about 96% of control compressive strength; the 10% mixture achieved about 86% of control flexural strength	Primarily physical and mechanical testing without chloride-related microstructural evaluation
Tong et al. [14]	Glass sand and glass powder used in a combined system	Several sizes and replacement contents	Optimized mixture reduced water absorption by 20.73% and chloride permeability by 63.10%; reported strength increases ranged from 12–45%	Combined aggregate and binder replacement rather than WGP replacing sand only
Bhat et al. [15]	Glass used as coarse aggregate, fine aggregate, and cement powder	0–25% at 5% intervals	Most favorable levels were approximately 15% for aggregate forms and 10% for powder	No chloride conditioning or embedded-steel evaluation
Gholampour et al. [17]	Glass sand replacing natural sand with GP, FA, and GGBS systems	GS: 25%, 50%, 100%	At 25%, compressive strength and modulus were only 3% and 2% below control; absorption decreased by 40%, 46%, and 51% at 25%, 50%, and 100%	Multi-material system; no direct steel-corrosion measurements
Son et al. [18]	Untreated and pretreated glass sand replacing all natural sand	100%	Pretreatment increased mechanical properties by up to 28% relative to untreated glass-sand concrete	Complete replacement and pretreated sand rather than untreated WGP below 75 μm
Wang et al. [19]	Waste-glass concrete under carbonation and chloride attack	Study-specific glass contents	Fine-grained glass sand increased compressive strength by 14.78%; chloride diffusion and surface enrichment were quantified	Coupled carbonation–chloride environment
Zhang et al. [20]	GP replacing cement in seawater-mixed steel-fiber mortar	25% cement replacement	ITZ thickness decreased from 45 to 35 μm; porosity decreased from 95% to 85%; chloride concentration decreased by 15–25%; corrosion was delayed by 3–6 cycles	Mortar, cement replacement, seawater mixing, and dispersed steel fibers
Kadhim and Muttar [21]	Green glass powder replacing cement under combined chloride–sulfate exposure	10%, 20%, 30%	The G20 sample achieved a compressive strength of 65.6 MPa after 28 days of severe exposure; the samples were initially treated with water for 28 days prior to subsequent exposure.	Cement substitution and combined exposure to chlorides and sulphates; the mechanical properties were compared with pre-exposure values after 28 days, in the absence of water-cured control specimens of similar total age

Present study	Untreated clear WGP below 75 μm replacing natural sand	0%, 5%, 10%, 15%, 20%	Equal-age mechanical comparison supported by water absorption, localized SEM/EDS, and qualitative embedded-steel observations	Chloride diffusion and corrosion rate are not quantified

Note: X-ray Diffraction (XRD), waste glass powder (WGP), sodium chloride (NaCl), Scanning Electron Microscopy (SEM), Energy-Dispersive X-ray Spectroscopy (EDS).

Table S2. Individual and mean compressive strength results

Mix ID	Glass Powder Replacement	Normal Water Specimens' Strength, MPa (28 days)	Normal Water Strength, MPa (28 days)	Normal Water Specimens' Strength, MPa (56 days)	Normal Water Strength, MPa (56 days)	NaCl Specimens' Strength, MPa (56 days)	NaCl Strength, MPa (56 days)
WGP0	0%	S1 = 35.32 S2 = 34.72 S3 = 35.39	35.14	S1 = 37.21 S2 = 37.29 S3 = 36.58	37.03	S1 = 36.34 S2 = 35.66 S3 = 36.27	36.10
WGP5	5%	S1 = 37.61 S2 = 36.90 S3 = 37.54	37.35	S1 = 40.35 S2 = 39.67 S3 = 40.43	40.15	S1 = 38.62 S2 = 38.69 S3 = 37.96	38.42
WGP10	10%	S1 = 46.13 S2 = 45.35 S3 = 46.22	45.90	S1 = 48.50 S2 = 47.58 S3 = 48.40	48.16	S1 = 47.23 S2 = 46.43 S3 = 47.32	46.99
WGP15	15%	S1 = 34.46 S2 = 34.53 S3 = 33.88	34.29	S1 = 35.83 S2 = 35.16 S3 = 35.76	35.58	S1 = 34.89 S2 = 34.30 S3 = 34.96	34.72
WGP20	20%	S1 = 31.25 S2 = 30.72 S3 = 31.31	31.10	S1 = 34.07 S2 = 34.14 S3 = 33.50	33.90	S1 = 32.84 S2 = 32.22 S3 = 32.77	32.61

Note: Waste glass powder (WGP), sodium chloride (NaCl).

Table S3. Individual and mean flexural strength results of WGP concrete under different curing and NaCl exposure conditions

Mix ID	Glass Powder Replacement, %	Normal Water Avg. Flexural Strength, MPa (28 days)	Normal Water Specimens' Flexural Strength, MPa (28 days)	Normal Water Avg. Flexural Strength, MPa (56 days)	Normal Water Specimens' Flexural Strength, MPa (56 days)	NaCl Avg. Flexural Strength, MPa (56 days)	NaCl Specimens' Flexural Strength, MPa (56 days)
WGP0	0	3.00	S1 = 3.02 S2 = 2.94 S3 = 3.04	3.20	S1 = 3.24 S2 = 3.14 S3 = 3.22	3.17	S1 = 3.18 S2 = 3.22 S3 = 3.11
WGP5	5	3.37	S1 = 3.42 S2 = 3.31 S3 = 3.38	3.39	S1 = 3.40 S2 = 3.44 S3 = 3.33	3.43	S1 = 3.49 S2 = 3.36 S3 = 3.44
WGP10	10	3.46	S1 = 3.48 S2 = 3.52 S3 = 3.38	3.59	S1 = 3.66 S2 = 3.51 S3 = 3.60	3.52	S1 = 3.53 S2 = 3.45 S3 = 3.58
WGP15	15	2.76	S1 = 2.77 S2 = 2.81 S3 = 2.70	2.93	S1 = 2.94 S2 = 2.86 S3 = 2.99	2.85	S1 = 2.91 S2 = 2.78 S3 = 2.86
WGP20	20	2.55	S1 = 2.56 S2 = 2.49 S3 = 2.60	2.70	S1 = 2.75 S2 = 2.64 S3 = 2.71	2.63	S1 = 2.64 S2 = 2.68 S3 = 2.57

Note: Waste glass powder (WGP), sodium chloride (NaCl).

Table S4. Individual and mean splitting tensile strength results of WGP concrete under different curing and NaCl exposure conditions

Mix ID	Glass Powder Replacement, %	Normal Water 28 Days Avg. ft, MPa	Normal Water 28 Days Specimens ft, MPa	Normal Water 56 Days Avg. ft, MPa	Normal Water 56 Days Specimens ft, MPa	NaCl Exposure 56 Days Avg. ft, MPa	NaCl Exposure 56 Days Specimens ft, MPa
WGP0	0%	2.22	S1 = 2.23 S2 = 2.17 S3 = 2.26	2.31	S1 = 2.35 S2 = 2.26 S3 = 2.32	2.27	S1 = 2.28 S2 = 2.31 S3 = 2.22
WGP5	5%	2.42	S1 = 2.47 S2 = 2.36 S3 = 2.43	2.55	S1 = 2.56 S2 = 2.60 S3 = 2.49	2.50	S1 = 2.51 S2 = 2.44 S3 = 2.55

			S1 = 2.71		S1 = 3.21		S1 = 2.92
WGP10	10%	2.70	S2 = 2.76	3.15	S2 = 3.08	2.91	S2 = 2.84
			S3 = 2.63		S3 = 3.16		S3 = 2.97
			S1 = 2.13		S1 = 2.24		S1 = 2.18
WGP15	15%	2.12	S2 = 2.16	2.20	S2 = 2.15	2.17	S2 = 2.12
			S3 = 2.07		S3 = 2.21		S3 = 2.21
			S1 = 1.74		S1 = 2.11		S1 = 1.93
WGP20	20%	1.73	S2 = 1.68	2.07	S2 = 2.02	1.92	S2 = 1.96
			S3 = 1.77		S3 = 2.08		S3 = 1.87

Note: Waste glass powder (WGP), sodium chloride (NaCl).

Table S5. Individual water absorption measurements of WGP concrete specimens

Mix ID	Specimen	Dry Mass A, g	Saturated Mass B, g	Absorbed Water B-A, g	Water Absorption, %
WGP0	1	2320	2440	120	5.17
WGP0	2	2310	2431	121	5.24
WGP0	3	2305	2423	118	5.12
WGP5	1	2315	2428	113	4.88
WGP5	2	2298	2407	109	4.74
WGP5	3	2308	2418	110	4.77
WGP10	1	2321	2413	92	3.96
WGP10	2	2312	2401	89	3.85
WGP10	3	2306	2394	88	3.82
WGP15	1	2302	2408	106	4.60
WGP15	2	2317	2425	108	4.66
WGP15	3	2309	2415	106	4.59
WGP20	1	2311	2428	117	5.06
WGP20	2	2297	2416	119	5.18
WGP20	3	2304	2421	117	5.08

Note: Waste glass powder (WGP).

Table S6. Local elemental compositions of the selected concrete regions obtained by EDS

Specimen	Exposure Condition	O, wt.%	Na, wt.%	Mg, wt.%	Al, wt.%	Si, wt.%	S, wt.%	K, wt.%	Ca, wt.%	Fe, wt.%	Zr, wt.%	I, wt.%	Total, wt.%
WGP0	Normal water	51.61	1.00	0.59	2.16	7.44	—	1.65	35.55	—	—	—	100.00
WGP0	NaCl exposure	51.13	13.62	—	1.08	7.94	—	0.90	24.56	0.77	—	—	100.00
WGP10	Normal water	49.25	1.14	0.71	3.54	16.56	—	2.23	23.66	2.90	—	—	100.00
WGP10	NaCl exposure	42.99	0.86	—	0.61	7.86	0.54	0.48	32.87	—	11.57	2.22	100.00

Note: Waste glass powder (WGP), Energy-Dispersive X-ray Spectroscopy (EDS), sodium chloride (NaCl).

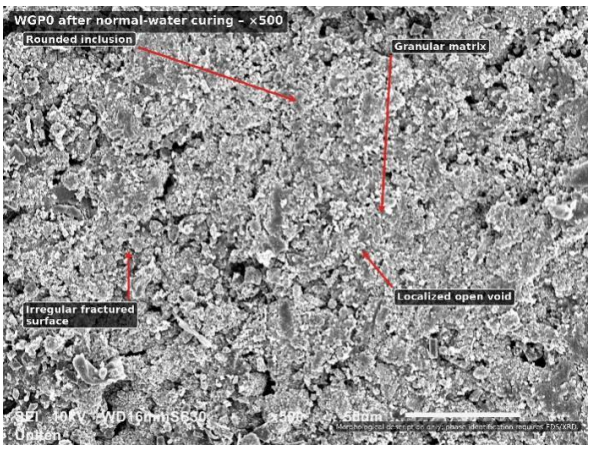

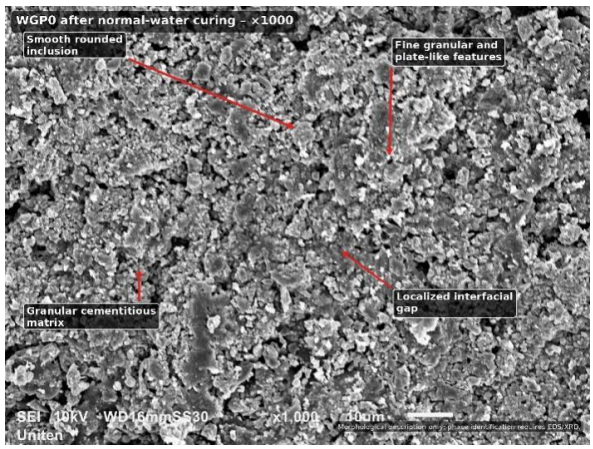

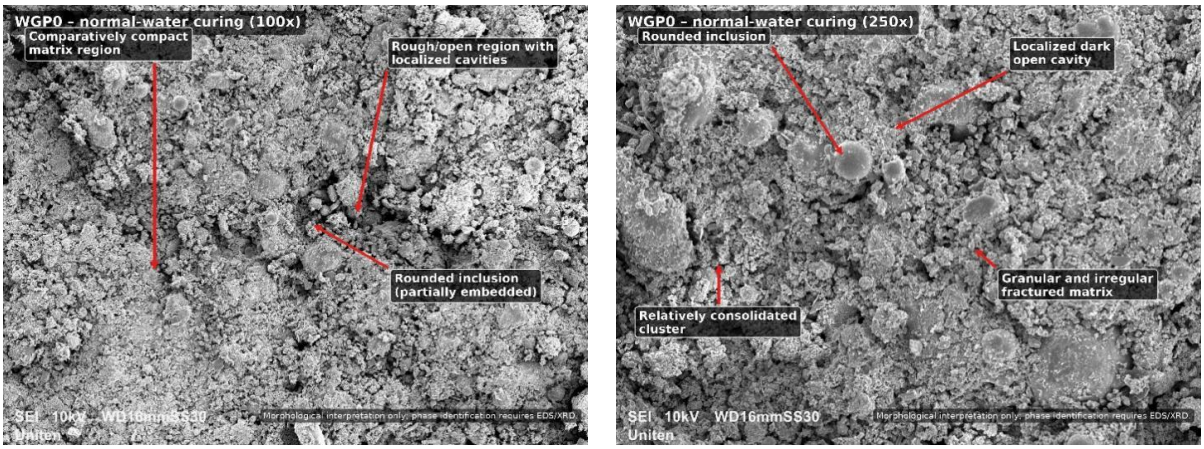

Figure S1. Additional Scanning Electron Microscopy (SEM) micrographs of waste glass powder 0 (WGP0) after normal water curing at different magnifications, complementing Figure 6

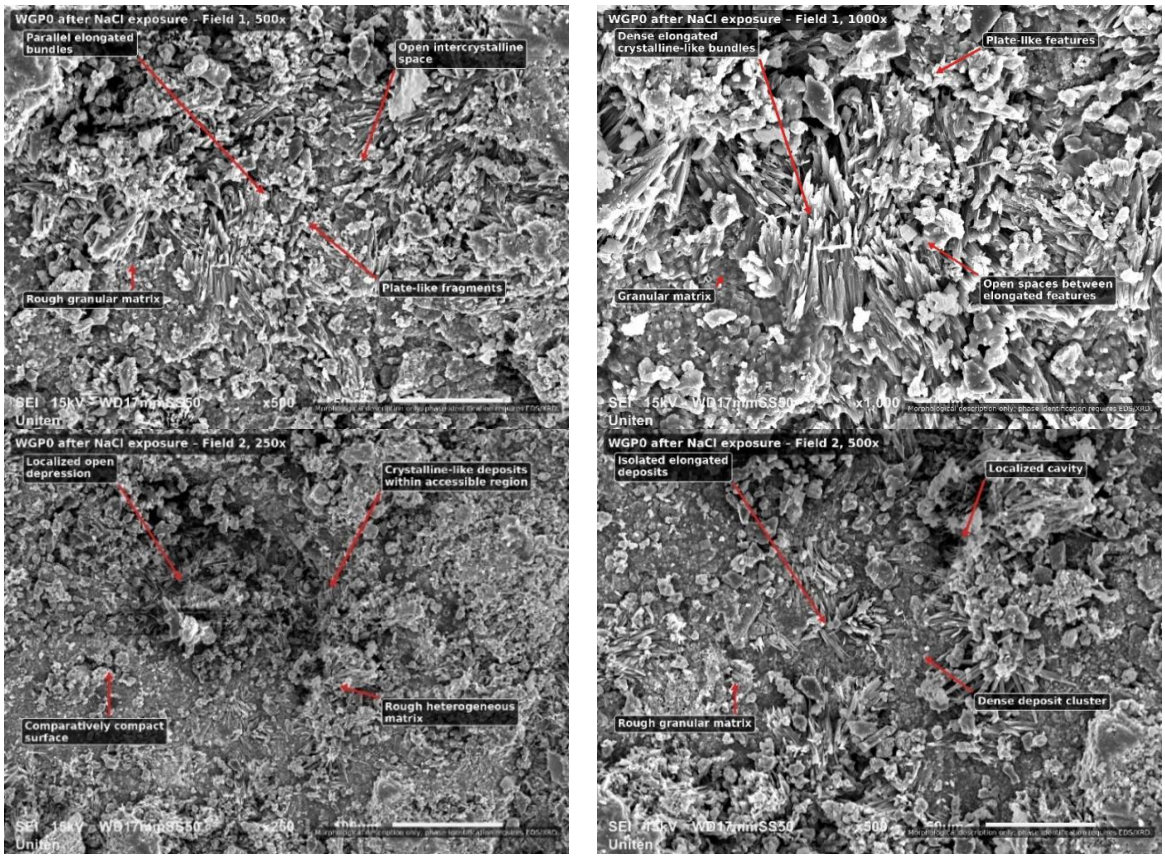

Figure S2. Additional Scanning Electron Microscopy (SEM) micrographs of waste glass powder 0 (WGP0) after sodium chloride (NaCl) exposure at different magnifications, complementing Figure 7

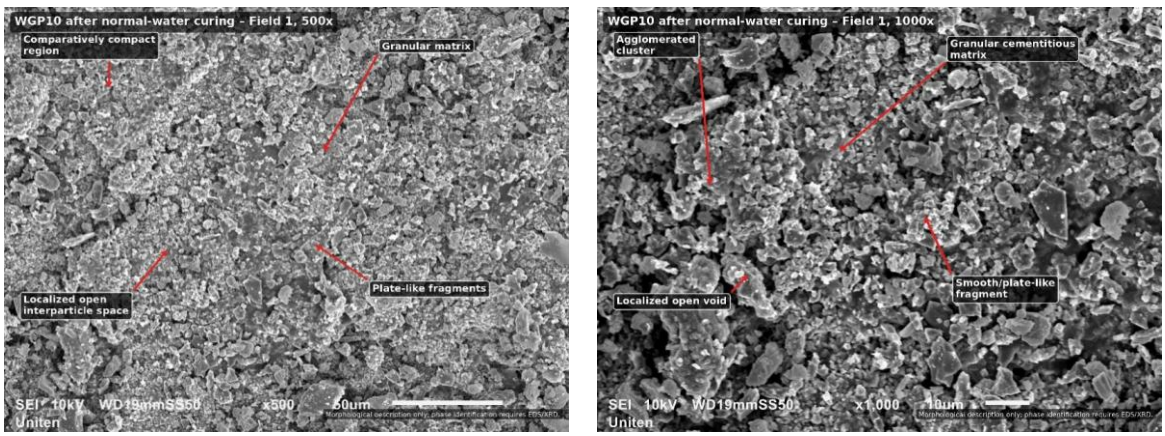

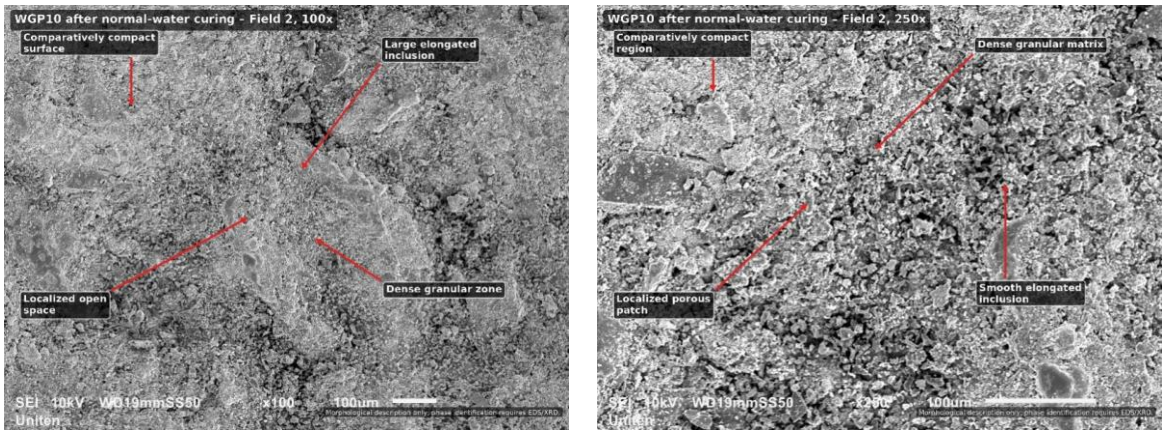

Figure S3. Additional Scanning Electron Microscopy (SEM) micrographs of waste glass powder 10 (WGP10) after normal water curing at different magnifications, complementing Figure 8

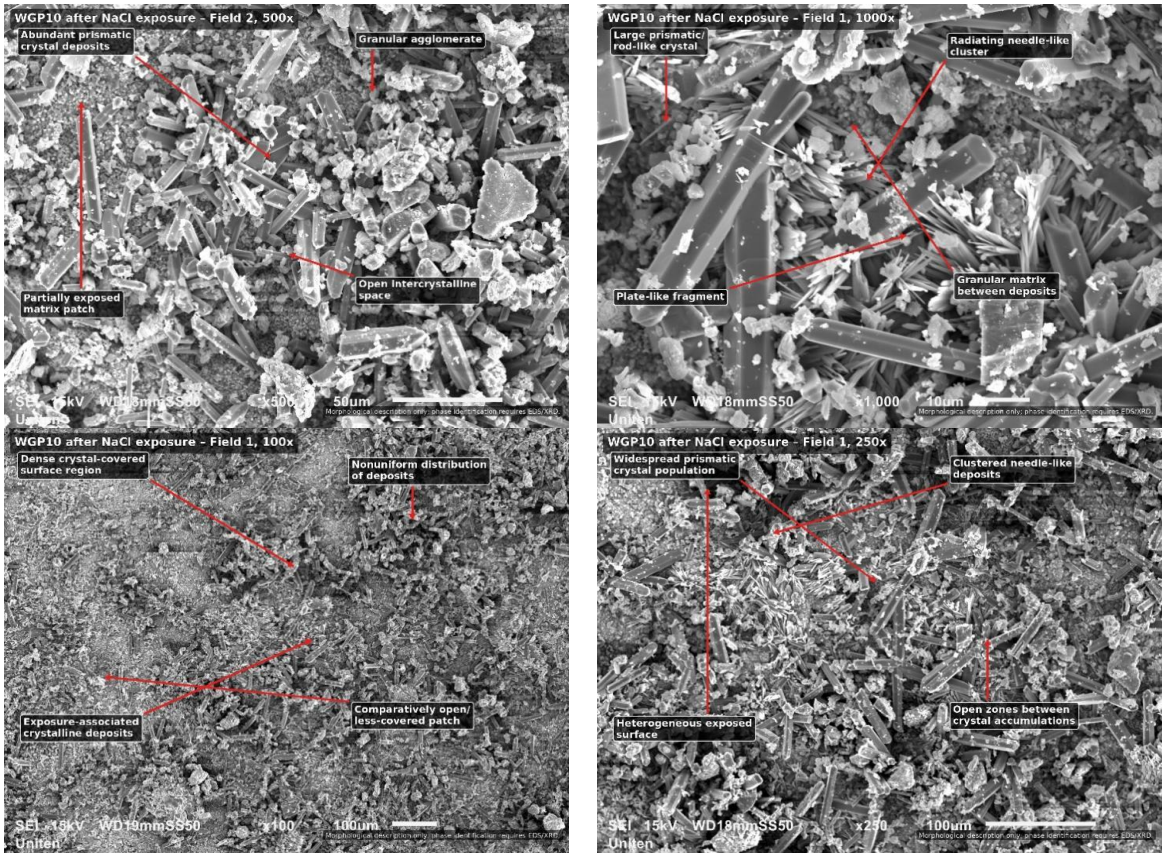

Figure S4. Additional Scanning Electron Microscopy (SEM) micrographs of waste glass powder 10 (WGP10) after sodium chloride (NaCl) exposure at different magnifications, complementing Figure 9